AN INVESTIGATION OF THE SYSTEM

WOLFRAM - COBALT - CARBON

By

Pekka Rautala

B. S. Helsinki Institute of Technology

1946

Submitted in Partial Fulfillment of the

Requirements for the Degree of

DOCTOR OF SCIENCE

from the

Massachusetts Institute of Technology

1951

Signature of Author
Department of Metallurgy
May 11, 1951

Signature of Professor
in Charge of Research

Signature of Chairman
Department Committee
on Graduate Research

Report Documentation Page

Form Approved
OMB No. 0704-0188

1. REPORT DATE	2. REPORT TYPE	3. DATES COVERED
11 MAY 1951		**00-00-1951 to 00-00-1951**

4. TITLE AND SUBTITLE	5a. CONTRACT NUMBER
An Investigation of the System: Wolfram - Colbalt - Carbon	5b. GRANT NUMBER
	5c. PROGRAM ELEMENT NUMBER
6. AUTHOR(S)	5d. PROJECT NUMBER
	5e. TASK NUMBER
	5f. WORK UNIT NUMBER
7. PERFORMING ORGANIZATION NAME(S) AND ADDRESS(ES) **Massachusetts Institute of Technology,77 Massachusetts Avenue,Cambridge,MA,02139-4307**	8. PERFORMING ORGANIZATION REPORT NUMBER
9. SPONSORING/MONITORING AGENCY NAME(S) AND ADDRESS(ES)	10. SPONSOR/MONITOR'S ACRONYM(S)
	11. SPONSOR/MONITOR'S REPORT NUMBER(S)

12. DISTRIBUTION/AVAILABILITY STATEMENT
Approved for public release; distribution unlimited

13. SUPPLEMENTARY NOTES

14. ABSTRACT

15. SUBJECT TERMS

16. SECURITY CLASSIFICATION OF:			17. LIMITATION OF ABSTRACT	18. NUMBER OF PAGES	19a. NAME OF RESPONSIBLE PERSON
a. REPORT **unclassified**	b. ABSTRACT **unclassified**	c. THIS PAGE **unclassified**	**Same as Report (SAR)**	**109**	

AN INVESTIGATION OF THE SYSTEM WOLFRAM-COBALT-CARBON

by Pekka Rautala

Submitted for the degree of Doctor of Science

in the Department of Metallurgy on May 11, 1951

The phases and phase equilibria in the system wolfram-cobalt-carbon have been studied by x-ray diffraction methods, metallographic technique and thermal analysis. An x-ray method is introduced for evaluating compositions and amounts of phases.

Diwolfram carbide is shown to possess a defect lattice with 8-21 percent of unoccupied carbon sites. Monowolfram carbide indicates a very narrow range of homogeneity. In addition to the carbide Co_3W_3C, reported previously the existence of double carbides $Co_3W_6C_2$ and $Co_3W_{10}C_4$ is revealed. Isomorphous carbides are shown to form in corresponding iron and nickel systems. The lattices are solved and the constants measured.

The carbide Co_3W_3C is shown to be stable, whereas monowolfram carbide is found to be metastable in alloys where wolfram-cobalt ratio is less than one.

Tentative diagrams of stable and metastable equilibrium in the system wolfram-cobalt-carbon are proposed. The basic reactions in sintering of cobalt cemented wolfram carbides are explained.

Table of Contents

List of Illustrations

List of Tables

Acknowledgement

To Professor John T. Norton the author wishes to express his appreciation and thanks for his encouragement, advice and guidance during this work, which was performed under his supervision.

Special thanks are extended to Mr. Geoffrey Munday for his cooperation in the development of the new x-ray intensity method, also to Mr. Kenneth Carlson and Mr. William Campbell for their assistance in the experimental work.

The author wishes to take this opportunity to thank Professor Morris Cohen for his friendly interest and valuable advice.

Part of this work was sponsored by the Ordnance Department of the United States Army, Contracts No. W-19-020-ORD-6489 and No. DA-19-020-ORD-10, under the technical supervision of Watertown Arsenal Laboratory. This support is deeply appreciated.

1. Introduction

The original purpose of this investigation was to study the constitution of cobalt cemented wolfram carbides. It has been generally accepted that the partial diagram Co-WC, on which all the industrially important carbides have their compositions, is a quasi-binary. It became evident in the course of the work that this was a mistaken premise. The work was therefore expanded to include the neighboring alloys and later the whole ternary diagram wolfram-cobalt-carbon. This study revealed new double carbides, previously unreported. It also became obvious that the general appearance of the ternary system depends on the wolfram-carbon binary diagram. There exist two carbides W_2C and WC in this system. The literature survey pointed out rather wide homogeneity range in W_2C but none in WC. The flexible W_2C structure could allow replacements of wolfram atoms by cobalt atoms and permit the formation of a series of double carbides.

The problem of the instability of the carbides in this system has a rather important role. During the course of the work it was reported by Brownlee[1] that W_2C is unstable.

Because of the important structural relationship between the double carbides and W_2C and its influence in understanding the ternary diagram, a careful study of the binary wolfram-carbon diagram was started. X-ray study by the lattice parameter method was used to determine the homogeneity range of W_2C but the single phase field of wolfram carbide was too narrow to be measurable by this method. It was hoped to settle the problem by intensity measurements but the first results were discouraging. A closer analysis

revealed a new method to locate solubility limits, and also offered a means for quantitative x-ray analysis. In connection with this work the segregation, which occurs during the preparation of the x-ray spectrometer specimens, had to be studied.

2. Summary

The phases and equilibria in the system wolfram-cobalt-carbon have been studied by x-ray diffraction methods, metallographic technique and thermal analysis. The specimens were prepared by sintering powder mixtures.

The composition range of diwolfram carbide has been determined by parametric and intensity methods. Diwolfram carbide is shown to possess a defect lattice with 8-21 percent of unoccupied carbon sites. The lattice constants of diwolfram carbide in Angstrom units are given by equations:

$$a = 5.1000 \times 10^{-3} \times b + 2.8363$$

$$c = 3.6429 \times 10^{-3} \times b + 4.6135$$

where b is the carbon content in atomic percent. The composition range of monowolfram carbide is very narrow and the lattice constants were measured as a = 2.9062 A and c = 2.8335 A.

The constitution diagram wolfram-carbon by Sykes[2] has been modified by the results of the present investigation.

An x-ray method is introduced to determine the compositions of the phase boundaries in equilibrium diagrams. The method is applicable for determination of the amounts of phases in powder specimens. The complications caused by segregation of phases in the specimens have been studied in a preliminary way.

The existance of two double carbides, called theta and kappa, has been revealed. The compositions correspond to formulae $Co_3W_6C_2$ and $Co_3W_{10}C_4$. The structure of the theta phase resembles that of the eta phase, Co_3W_3C. The lattice is face centered cubic and the lattice constant 11.25A. The kappa phase has hexagonal lattice; the axes were measured as a = c = 7.848 A.

These phases were found to form by peritectic reactions:

$$\text{Liquid} + W_2C + W = K \text{ and Liquid} + K + W = \theta.$$

Isomorphous phases were shown to form in the corresponding iron and nickel systems.

The eta phase Co_3W_3C, was found to be stable, whereas monowolfram carbide is metastable in alloys, where the wolfram-cobalt ratio is less than one.

Tentative diagrams of stable and metastable equilibrium in the system wolfram-cobalt-carbon have been proposed. The quasi-binary diagram cobalt-wolfram carbide, usually assumed, is shown to be incorrect. The basic reactions in sintering cobalt cemented wolfram carbides have been explained.

3. Previous Investigations

The literature contains a great many references to the wolfram-cobalt-carbon system, but only those have been reviewed here which seem to have some significant bearing on the constitution of the ternary diagram.

The binary diagrams cobalt-carbon, cobalt-wolfram and wolfram-carbon are available in the Metals Handbook[3] as formulated by Sykes.

It is generally accepted that no stable carbides form in the cobalt-carbon system. Two unstable carbides have been reported. One of formula Co_3C is first mentioned by Ruff and Keilig[4] and later by Schenck and Klas[5] and Hofer and Peebles[6]. A carbide of formula Co_2C has been proposed by Bahr and Jensen[7].

The eutectic reaction: Liquid-beta-graphite, where beta is the cobalt solid solution, occurs at about 1300°C. This value is due to Boecker[8] whereas Takeda[9] reports 1315°C. The carbon solubility of beta at the eutectic temperature has been reported between 0.81 and 1.1 percent by weight.

In the cobalt-wolfram system there exist two intermediate compounds, gamma and delta. According to several investigators, Sykes[10], Koster and Tonn[11] and Takeda[9] gamma has the formula Co_7W_2. Magneli and Westgren[12] who have solved the structure of the gamma phase, prefer the formula Co_3W. The peritectoid reaction, beta + delta = gamma, which occurs at 1100°C has been reported as very sluggish. The delta phase has approximate composition CoW. Magneli and Westgren[12], who also have determined the structure of the delta phase, consider formula Co_7W_6 better. The delta phase is formed by a peritectic reaction, liquid + wolfram = delta. The temperature of this reaction has been reported as 1690°C by Sykes[10] and 1630°C by Takeda[9].

In addition to the reactions mentioned there exists an eutectic reaction, liquid = beta + delta at 1465°C.

Wolfram forms two carbides, mono and diwolfram carbides, discovered by Williams[13] and Moissan[14]. Monowolfram carbide was studied by Westgren and Phragmen[15], diwolfram carbide mainly by Becker[16]. Monowolfram carbide decomposes at 2600°C by a peritictic reaction WC = liquid + graphite. Sykes[2] has reported two eutectics: Liquid = WC + W_2C at 2525°C and liquid = W_2C + W at 2475°C. The homogeneity range of diwolfram carbide has been left open. Other solubilities are negligible. Measurements of the wolfram rich solubility limit of diwolfram carbide have been made by Horsting[17] but his results are inconsistant.

The only ternary phase reported in the wolfram-cobalt-carbon system is of composition Co_3W_3C and called eta (η). It was first studied by Adelskold, Sundelin and Westgren[18], although the isomorphous iron-wolfram double carbide was known earlier.

The eta phase has been considered unstable by Takeda[19] and Westgren[18]. The homogeneity range of eta is wide and opinions diverge whether there exist one or two eta phases. Two eta phases have been reported by Kislyokova[20] and Sandford and Trent[21], whereas one phase by Franssen[22] and Brownlee[1].

The section cobalt - monowolfram carbide has been studied by Wyman and Kelley[23] and a quasi binary diagram has been published by Sandford and Trent[21]. The solubility of cobalt in monowolfram carbide has been measured at Krupp-Widia Works[24] as about 0.2 percent at 1400°C.

A ternary equilibrium diagram wolfram-cobalt-carbon has been published by Takeda[9]. Both stable and metastable equilibria have been considered.

In the metastable system one ternary phase, eta, is formed by reaction:

$$\text{Liquid} + W_2C = \eta + W$$

The lines of two-fold saturation are shown only partically and it seems impossible to complete the diagram without violating the phase theory. The same can be said about the stable system which consists of no ternary phases.

4. Specimen Preparation

The alloys used in the present investigation were made from powders of wolfram, wolfram monocarbide, cobalt and carbon and were of the grade used in manufacture of commercial cemented carbides.

The wolfram and wolfram carbide were obtained from Fansteel Metallurgical Corporation. The carbon content of the wolfram carbide was shown by analysis to be 6.15 percent carbon by weight.

The cobalt powder was obtained from Carboloy Company and its analysis is reported in Table I.

The carbon was spectroscopic carbon of very high purity.

In general, the specimens had a weight of ten grams and the powders were weighed out to the nearest milligram. They were ground and mixed in small stainless steel ball mills, using balls of the same material. Ten milliliters of benzene was used as a dispersing agent. The mixing period was one hour since this was shown to give sufficiently good mixing of the powders without too great a contamination from the mill. After ball milling, the specimens were pressed in cylindrical or rectangular dies. No paraffin or other lubricant was used and the small compacts had sufficient green strength to be handled without difficulty.

Several sintering furnaces were employed. The most satisfactory arrangement was a vacuum furnace based on Arsem principle which employed a graphite helix as the resistance heating element. Specimens were placed on either graphite or zirconia stands and there was generally a slight carburization or decarburization of the specimen surface, depending on the

carbon content of the alloy. The evaporation of the cobalt at a sintering temperature of 1400°C was not significant, but became severe at 1500°C and up. The sintering time was one hour at 2000°C and 2 to 4 hours at lower temperatures. It was not possible to quench the specimens, but the cooling rates are rather fast as shown in Table II. In the system under investigation, the reactions are sluggish, and it is believed that the high temperature structures are satisfactorily retained.

If a series of alloys was employed for quantitative measurements the calculations were based on the chemical analysis of the sintered specimens. Qualitative surveying work is based on the original compositions and only a few specimens, picked at random, were analysed chemically.

Table I

Chemical Analysis of Cobalt

(PM 122 Carboloy)

Percent by Weight

Co - 98.6	O - 0.83
Ni - 0.28	Si - 0.15
Fe - 0.07	C - 0.045
Mn - 0.05	S - 0.044
Cu - Trace	

Table II

Cooling Rate in Arsem Vacuum Furnace

Time - minutes	Temperature °C
0	1351
1	1090
2	925
3	834
4	764
5	702

5. X-Ray Techniques

There are two general applications of x-ray technique to the problem of the ternary diagram. One has to do with the question of identification of the phase or phases in a particular specimen and this is done in the conventional manner of identifying the pattern of diffraction lines, which is characteristic of each of the possible phases. For this purpose the records obtained from the Norelco recording x-ray spectrometer are especially suitable and the standard techniques supply the necessary precision.

The other application is concerned with the determination of the composition limits of the single phase field and is especially important in the binary systems which form the basis of the ternary diagram. If the single phase fields have a considerable range of homogeneity, the well known parametric method is applicable and will yield the necessary precision. However, if the field is very narrow, this method does not apply and the conventional disappearing phase method is not sufficiently precise. Consequently it has been necessary to develop a new method which has the necessary precision and which will be applicable to this problem. The development has involved a considerable fraction of time spent on the research as a whole but its success has indicated applications of a much wider scope than the present problem.

The following sections indicate the application of these two techniques to the determination of the composition limits of the phases W_2C and WC.

5.1 The Parametric Method

The powder patterns were taken by a 10 centimeter symmetrical focussing camera. Using cobalt K alpha radiation, the camera recorded three diffraction line doublets, 12·1, 11·4 and 12·2, of the W_2C pattern. Because the structure of W_2C is hexagonal[16], Cohen's[25] analytical method had to be used in the calculations of the lattice constants. In Appendix I a sample calculation of one film is given.

5.11 Lattice Constants of W_2C

The compositions of the alloys and the measured lattice constants are given in Table III and represented graphically in Figure 1.

Within the single phase field, there was not enough evidence to detect deviation from Vegard's law.

The straight lines through the points have the following equations:

$$a = 5.1000 \times 10^{-3} \times b + 2.8363$$

$$c = 3.6429 \times 10^{-3} \times b + 4.6135$$

$$c/a = -1.3714 \times 10^{-3} \times b + 1.6210$$

Where b is the carbon content in percent* and a and c are the lattice constants of W_2C in Angstrom Units.

Within the two-phase fields, W + W_2C and W_2C + WC, the lattice constants should have constant values and were therefore obtained by averaging. The lattice constants of W_2C in two phase fields are given in Table IV.

---

* If not specified, the percentages in this work will be expressed on an atomic basis.

Table III

Lattice Constants of W_2C

Angstrom Units

Temperature 1425°C	Atomic % Carbon	a	c	c/a
	25.0	2.9947	4.7269	1.5784
	29.5	2.9949	4.7263	1.5781
	30.0	2.9948	4.7273	1.5785
	30.5	2.9943	4.7268	1.5786
	31.0	2.9938	4.7261	1.5786
	31.5	2.9969	4.7281	1.5777
	32.0	2.9977	4.7386	1.5774
	32.5	2.9967	4.7284	1.5779
	33.0	2.9973	4.7287	1.5777
Temperature 2000°C	28.5	2.9907	4.7234	1.5794
	29.0	2.9912	4.7234	1.5791
	29.5	2.9901	4.7233	1.5796
	30.5	2.9922	4.7246	1.5790
	31.0	2.9940	4.7266	1.5787
	31.0	2.9941	4.7263	1.5785
	31.5	2.9971	4.7284	1.5777
	32.0	2.9982	4.7292	1.5773
	32.5	2.9981	4.7292	1.5774
	33.0	2.9973	4.7289	1.4777
	33.0	2.9975	4.7285	1.5775

Figure 1

Lattice Constants of Diwolfram Carbide

The solid circles correspond to sintering temperature of 1425°C, the open circles of 2000°C.

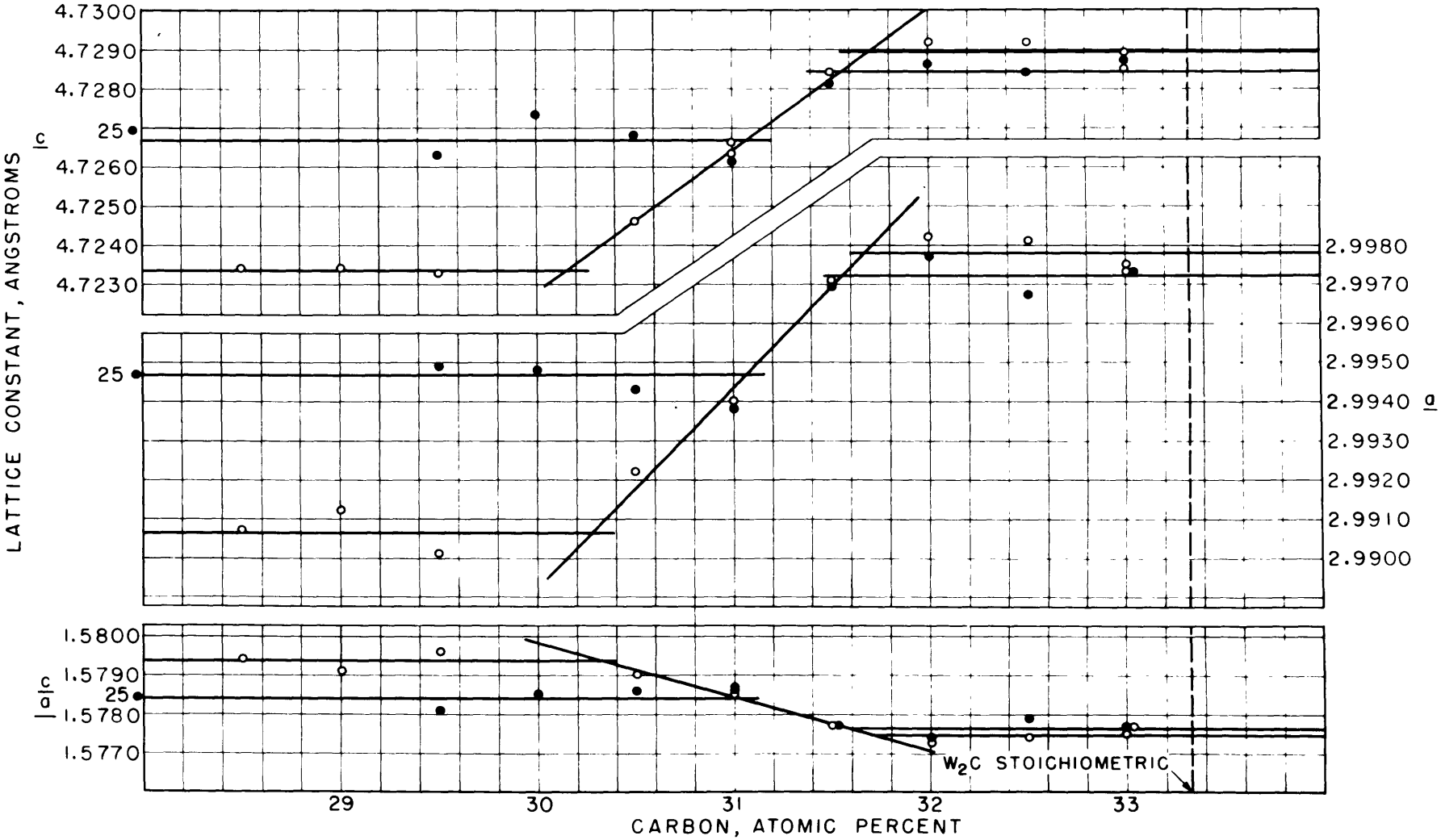
LATTICE CONSTANT, ANGSTROMS
c
4.7300
4.7290
4.7280
25
4.7260
4.7250
4.7240
4.7230
25
2.9980
2.9970
2.9960
2.9950
2.9940
a
2.9930
2.9920
2.9910
2.9900
c/a
1.5800
1.5790
25
1.5780
1.5770
W2C STOICHIOMETRIC
29
30
31
32
33
CARBON, ATOMIC PERCENT

FIGURE 1

5.12 Solubility Limits of W_2C

The values of a, c and c/a from Table IV were substituted into the equations on page 12, to give the solubility limits. Table V gives three values for each limit as obtained from the three equations. All these three values should be equal and are therefore averaged. Because the chemical determination of carbon showed more scattering than could be allowed, the results of analyses were averaged. An over-all decarburization of the series was 0.122 percent carbon . The solubility limits corrected by this value are given in the last column of Table V.

These results indicate that the stoichiometric carbon content, 33.33 percent, could not be reached. The solubility of carbon into W_2C increased very little with temperature 0.13 percent from 1425°C to 2000°C and can be considered as constant.

On the other hand the solubility of wolfram increases rapidly. This means that the homogeneity range of W_2C at room temperature has to be very narrow. Assuming it zero the solubility limit at eutectic temperature, 2475°C by extrapolation becomes about 28.5 percent of carbon.

Table IV

Lattice Constants of W_2C Saturated by W or by C

Angstrom Units

Field	Temperature °C	a	c	c/a
W + W_2C	1425	2.9947	4.7267	1.5784
W + W_2C	2000	2.9907	4.7234	1.5794
W_2C + WC	1425	2.9972	4.7286	1.5777
W_2C + WC	2000	2.9978	4.7290	1.5775

Table V

Solubility Limits of W_2C

Atomic Percent Carbon

Saturated by	Temperature °C	Determined from			Average	Corrected by Analysis
		a	c	c/a		
W	1425	31.064	31.066	31.012	31.047	30.93
W	2000	30.278	30.157	30.334	30.256	30.13
C	1425	31.539	31.585	31.574	31.566	31.44
C	2000	31.667	31.689	31.712	31.689	31.57

5.13 Solubility Limits of WC

A series of experiments, similar to those of W_2C, was performed in order to locate the solubility limits of WC. The x-ray technique used was the same, except that 12.0 and 20.2 and 12.1 reflections of WC were measured. The results are summarized in Table VI.

There seems to be no systematic trend in the values of Table VI, and the scatter is within the limits of the experimental errors. The homogeneity range of wolfram carbide, therefore, must be very narrow.

The average values of the lattice constants in Table VI should serve as good values of the lattice constants for wolfram carbide.

It is obvious that in this series of measurements the lattice parameter method yields no information as to the composition of wolfram carbide. The single phase alloy might be anywhere within the composition range studied. The measurements by intensity methods will be discussed in the next chapter.

Table VI

Lattice Constants of WC

Angstrom Units

Temperature 1400°C.	Percent Carbon	a	c	c/a
	48.0	2.9063	2.8335	.9750
	49.0	2.9064	2.8337	.9750
	50.0	2.9068	2.8335	.9748
	51.0	2.9060	2.8328	.9748
	51.0*	2.9062	2.8329	.9748
	52.0	2.9061	2.8341	.9752
	52.0*	2.9061	2.8342	.9753
	52.0**	2.9060	2.8335	.9750
	Average	2.9062	2.8335	.9750

* Duplicate measurement of the same specimen.

** Different specimen

5.2 A New Method to Determine Solubility Limits

5.21 Theoretical

Consider a polycrystalline two phase alloy of composition b. If the two phases are called α and β, the ratio of the amounts of the two phases are given by the lever rule:

$$\frac{m_\beta}{m_\alpha} = \frac{b - b_1}{b_2 - b} \qquad (1)$$

where b_1 and b_2 are the solubility limits at the temperature under consideration.

Each phase has its own characteristic x-ray spectrum. The intensity of a diffraction line is given by the equation[26]:

$$I = \frac{I_o}{16\pi R} \frac{e^4}{m_e^2 c^4} \lambda^3 \frac{FF^*_\beta j_\beta}{V^2_{a\beta}} \left(\frac{1 + \cos^2 2\theta}{\sin 2\theta \sin\theta}\right)_\beta V_\beta \qquad (2)$$

where

I_o = Intensity of primary beam

R = Spectrometer radius

e = Electronic charge

m_e = Electronic mass

c = Velocity of light

λ = Wavelength of x-ray beam

FF* = Structure factor

j = Multiplicity

V_a = Volume of the unit cell

θ = Bragg angle

$\frac{1 + \cos^2 2\theta}{\sin 2\theta \sin\theta}$ = (L.P.) = Lorentz - Polarization factor

V = Volume of the specimen.

Substituting the mass over density ratio for the volume, and using the x-ray density, the equation can be simplified to

$$I_{\beta\,(hkl)} = k_\beta \; m_\beta \qquad (3)$$

where

$$k_\beta = \frac{I_o}{1.6606 \times 16\pi R} \; \frac{e^4}{m_e^2 c^4} \; \lambda^3 \frac{FF^*_\beta \; j_\beta}{(V_a)^2_\beta \; (\Sigma\mu)_\beta} \; (L.P)_\beta$$

In this expression $\Sigma\mu$ is the molecular weight.

Equation (3) is valid for any phase and therefore the intensity ratio of two lines is:

$$\frac{I_{\beta(hkl)}}{I_{\alpha(h^1k^1l^1)}} = r \frac{m_\beta}{m_\alpha} \qquad (4)^*$$

r is the ratio of k_β to k_α and its value is:

$$r = \frac{FF^*_\beta \; j_\beta \; (L.P)_\beta}{FF^*_\alpha \; j_\alpha \; (L.P)_\alpha} \; \frac{(V_a)_\alpha}{(V_a)_\beta} \; \frac{(\Sigma\mu)_\alpha}{(\Sigma\mu)_\beta} \qquad (5)$$

r in general is a function of the indeces, but for each pair of diffraction lines it is a constant.

Substition of the mass ratio from equation (1) into equation (4) gives the intensity ratio z ($= I_\beta / I_\alpha$) as a function of the composition

$$z = r \frac{b - b_1}{b_2 - b} \qquad (6)$$

Equation (6) represents an equilateral hyperbola, which has assymptotes $z = -r$ and $b = b_2$. This can be seen, if the equation is written in the form:

$$z^1 \; b^1 = c$$

where $z^1 = z + r$, $b^1 = b - b_2$ and $c = r(b_1 - b_2)$. z becomes zero when $b = b_1$ and infinite if $b = b_2$. The solubility limits therefore are found by extrapolating the curve (6) to zero and infinite z. The slopes at the boundaries are finite and infinite respectively:

$$\left(\frac{dz}{db}\right)_{b = b_1} = \frac{r}{b_2 - b_1} \; ; \quad \left(\frac{dz}{db}\right)_{b = b_2} = \infty$$

---

*Note: Extinction effects will be negligible in powder specimens. Absorption errors are small also, because both diffracted beams have the same wavelength and travel through the same mixture of phases.

5.22 Analytical Determination of Limits

The analytical extrapolation can conveniently be carried out by the Gauss' least square method. Two new equations

$$\frac{\partial(\Sigma \Delta^2)}{\partial b_1} = o \text{ and } \frac{\partial(\Sigma \Delta^2)}{\partial b_2} = o \qquad (7)*$$

are formed from which the solubility limits can be obtained. In equations (7) Δ is the accidental deviation of an experimental point from the curve (6). The solution of equations (7) is given in Appendix II. The solubility limits are:

$$b_1 = \frac{\Sigma z^2 [\Sigma bz + r \Sigma b] - \Sigma z [\Sigma bz^2 + r \Sigma bz]}{r [n \Sigma z^2 - (\Sigma z)^2]}$$

$$b_2 = \frac{n [\Sigma bz^2 + r \Sigma bz] - \Sigma z [\Sigma bz + r \Sigma b]}{[n \Sigma z^2 - (\Sigma z)^2]} \qquad (8)$$

where n is the number of the experimental points.

The solutions (8) are formed by assuming that r is known. The value of r can be calculated by equation (5). In the case of unknown structures, where FF* is not available, it is necessary to solve r from experimental values. This can be done by forming a third equation (7):

$$\frac{\partial(\Sigma \Delta^2)}{\partial r} = o$$

and solving the three simultaneous equations. In this case the solutions become:

$$b_1 = \frac{\Sigma bz [(\Sigma bz)^2 - \Sigma z \Sigma b^2 z] + \Sigma b [\Sigma z^2 \Sigma b^2 z - \Sigma bz \Sigma bz^2] + \Sigma b^2 [\Sigma z \Sigma bz^2 - \Sigma bz \Sigma z^2]}{\Sigma z [(\Sigma bz)^2 - \Sigma z \Sigma b^2 z] + n [\Sigma z^2 \Sigma b^2 z - \Sigma bz \Sigma bz^2] + \Sigma b [\Sigma z \Sigma bz^2 - \Sigma bz \Sigma z^2]}$$

$$b_2 = \frac{\Sigma bz [\Sigma z \Sigma b^2 - \Sigma bz \Sigma b] + \Sigma bz^2 [(\Sigma b)^2 - n \Sigma b^2] + \Sigma b^2 z [n \Sigma bz - \Sigma z \Sigma b]}{\Sigma z [\Sigma z \Sigma b^2 - \Sigma bz \Sigma b] + \Sigma z^2 [(\Sigma b)^2 - n \Sigma b^2] + \Sigma bz [n \Sigma bz - \Sigma z \Sigma b]} \qquad (8a)$$

$$r = \frac{\Sigma z [(\Sigma bz)^2 - \Sigma z \Sigma b^2 z] + n [\Sigma z^2 \Sigma b^2 z - \Sigma bz \Sigma bz^2] + \Sigma b [\Sigma z \Sigma bz^2 - \Sigma bz \Sigma z^2]}{\Sigma z [\Sigma z \Sigma b^2 - \Sigma bz \Sigma b] + \Sigma z^2 [(\Sigma b)^2 - n \Sigma b^2] + \Sigma bz [n \Sigma bz - \Sigma z \Sigma b]}$$

From equations (8a) b_1 and b_2 will be obtained without solving for r at all. Thus r merely serves as a check of calculations in case it can be evaluated theorectically. Actually the solution for r can be obtained without any further calculations, because its value is simply the ratio of the denominators of b_1 and b_2 in equations (8a)

* Note: Instead of writing $\sum_i \Delta_i^2$, the simpler notation $\sum \Delta^2$ is used.

5.23 Graphical Determination of Limits

If the constant r is known, it is possible to find b_1 and b_2 graphically. The extrapolation technique, however, is too uncertain. It follows from the properties of an equilateral hyperbola that the distances from the point of tangency (b_o, z_o) to both assymptotes are equal, if the slope is unity. A simple analysis, carried through in Appendix III gives

$$b_1 = b_o - z_o - \frac{z_o^2}{r}$$

$$b_2 = b_o + z_o + r \qquad (9)$$

It is not easy to locate the point (b_o, z_o) accurately because of the scatter of the experimental points. However the method is fast if high precision is not required. By chosing a pair of lines, which for pure phases have approximately equal intensities, the constant r is not far from unity. Expressing the composition in proper units, the error due to r is small and of the same order as the uncertainty in b_o.

5.24 Limitations due to Segregation. Quantitative Analysis

In the method just explained one is dealing with two-phase alloys. If single powder particles consist of one phase only, the phases may separate during the spectrometer specimen preparation. For spherical particles the settling velocity according to Stokes' law, is proportional to the square of the particle radius and to the difference of the densities of the particle and liquid: $v \approx r^2 (\rho - \rho_o)$. The coarser and heavier phase will therefore segregate on the bottom. If a two phase alloy in pulverizing breaks so that single particles consist of two phases, this segregation does not exist. The segregation phaenomenon is easier to study in the case of a mechanical mixture, where the solubility limits are zero and

one hundred percent respectively. The basic equation (6) now reduces to :

$$z = r \frac{b}{100-b} \qquad (10)$$

Equation (10) should give uniquely the amounts of both phases from the measured intensity ratio. In general this is not true. r can be calculated either by equation (5) or from experimentally measured intensities by equation :

$$r = \frac{\Sigma b\ z\ (100-b)}{\Sigma b^2} \qquad (11)$$

It is found, that this r and the value of r from equation (5) disagree, the difference being due to the segregation.

The x-rays are diffracted mainly by the surface of the specimen. If the phase, which segregates on the bottom of the specimen, is called α the diffracting layer will show pure β at some overall composition b_s. The effect of this segregation is to change the apparent solubility limit from 100 to b_s. The other limit still is zero, because, if there is no β present, the intensity of any β phase line will be zero. Therefore the equation (6) can be written into form :

$$z = r \frac{b}{b_s - b} \qquad (12)$$

If r from equation (5), which should be the proper one, is used, the factor b_s is given by:

$$b_s = \frac{\Sigma b\ z^2 + r\Sigma b\ z}{\Sigma z^2} \qquad (13)$$

Again it is possible to get another set of solutions

$$b_s = \frac{\Sigma b^2 z \Sigma bz - \Sigma b\ z^2 \Sigma b^2}{(\Sigma bz)^2 - \Sigma b^2 \Sigma z^2}$$

$$r = \frac{\Sigma b^2 z \Sigma z^2 - \Sigma bz \Sigma b\ z^2}{(\Sigma bz)^2 - \Sigma b^2 \Sigma z^2} \qquad (14)$$

Because of the second order effects the values of r (5) and r (14) might differ. The deviations apparently are more severe, if low diffraction angles are used. For high diffraction angles, where the x-ray beam penetrates appreciably deeper, the agreement should be good.

The composition of an unknown mixture can be obtained from the following equation:

$$b = \frac{b_s}{z + r} \times z \qquad (15)$$

by measuring the intensity ratio z for that specimen. Equation (15) is of such a form that the value of r does not critically effect the final result.

5.24 Segregation Experiments

To check the theory represented in the previous chapter, a series of experiments were carried out. The components of the mixture, W and WC, were chosen in the same system, in which the solubility limits were due to be determined. Three mixtures were prepared by ball milling.

The compositions of the specimens and the measured intensity ratios are given in the following table:

WC at. %	$I_{WC10.1}/I_{W110}$	$I_{WC11.2}/I_{W310}$	$I_{WC30.1}/I_{W321}$
25.2	.235	.201	.104
44.4	.583	—	—
51.6	.851	.740	.385

The intensities were measured by automatic, slow speed, recording x-ray spectrometer. The integrated intensity is proportional to the area under the curve, and was measured by weighing the cut out paper.

The results of calculations by different equations are summarized in Table VII. The evaluation of the theoretical r is given in Appendix IV.

Table VII shows that the simple equation (10) in combination with r from equation (5) cannot be used as such. The deviations are due to the segregation and even the high angle reflections, where the penetration depth is large, give incorrect results.

The solutions by equations (10) and (11) are appreciably better. In this case the z vs. b curve is allowed to adjust itself through the points, and only the limits are fixed. The curve (10), (11) does not therefore, have the theoretical shape. This can be seen in the fact that higher angle technique does not improve the results.

The two last methods, (5)(12)(13) and (14)(15) give good results especially if high angle reflections are used.

It is interesting to note that the values of b, obtained by method (5)(10) will yield the solutions (5)(12)(13), if multiplied by b_s from (5)(25)(13). Thus these b_s values could be called segregation factors. This segregation factor is a function of the diffraction angle. If $b_s(\theta)$ is extrapolated to $\theta = 90$ degrees, it approaches unity. Only in very thin specimens, where the x-ray beam passes back and forth through the whole specimen b_s may become equal to one.

The value of $b_s(\theta)$ depends on the spectrometer specimen preparation, which therefore should be standardized. Referring to Stokes' law it is seen that the segregation is decreased if the time allowed for it is shortened. The specimen preparation, however, does not require special equipment.

Table VII

Results of Segregation Experiments

b_1, b_2 and b_3 refer to the carbon content of the three specimens.

Equations Used	Reflections Used	r	b_s	b_1	b_2	b_3
(5) (10)	10.1/110	.444	100	34.6	56.8	65.7
	11.2/310	.399	100	33.5	-	65.0
	30.1/321	.245	100	29.8	-	61.1
(10) (11)	10.1/110	.761	100	23.6	43.4	52.8
	11.2/310	.675	100	22.9	-	52.3
	30.1/321	.351	100	22.9	-	52.3
(5) (12) (13)	10.1/110	.444	78.1	27.0	44.3	51.3
	11.2/310	.399	79.1	26.5	-	51.4
	30.1/321	.245	84.4	25.18	-	51.60
(14) (15)	10.1/110	.535	84.3	25.7	44.0	51.8
	11.2/310	.474	84.7	25.22	-	51.62
	30.1/321	.244	84.3	25.19	-	51.59
	Original compositions			25.20	44.40	51.60

Normal care and fast drying allows one to prepare consistant specimens. The b_s values from equations (14) and (15) are independent of the diffraction angle. This is so because the curve (15) was allowed to deviate from the theoretical shape. There, however, it is interesting to notice that for high angle reflections the curve (15) attains the theoretical shape, as indicated by the values of r and b_s.

It might be mentioned here that the method described above may offer a rapid means to study the particle size of a powder. Mixtures of known particle sizes with standard powder should yield a master plot of segregation factors as a function of particle sizes. An unknown particle size could then be determined by measuring its segregation factor.

5.26 Solubility Limit Determination of W_2C and WC by the New Method

A series of four specimens was prepared in the usual manner of WC and W powders. The sintering was one hour at 2000°C. The sintered specimens were analysed for carbon and the intensity ratio of $WC_{10.1}$ and $W_2C_{10.1}$ lines were measured by spectrometer. The integrated intensity was measured in three different ways:

a. Scanning with a motor driven Geiger Counter over the diffraction line,

b. Point counting the line,

c. Using automatic recording.

The intensities measured by all these methods were consistant. The average intensity ratios are given in Table VIII.

From these experimental data the solubility limits can be determined by different methods as explained earlier. Table IX summarizes the results of the calculations, which are given in Appendix V.

Table VIII

Experimental Intensity Ratios of WC + W_2C Alloys

b = Weight percent Carbon	z = $I_{WC_{10.1}}/I_{W_2C_{10.1}}$
3.68	.2586
4.19	.5437
4.57	.8447
5.13	1.7032

Table IX

Solubility Limits of W_2C and WC at 2000°C.

Method Used	r	Percent Carbon	
		b_1 = C rich W_2C	b_2 = C poor WC
(5)(8)	.848	31.302	50.498
(8a)	.857	31.356	50.532
Graphical	.848	31.9	50.4
Lattice Parameter	-	31.57	-

The results given in Table IX show that all methods give consistant results. The graphical method is, as expected, less accurate. Figure 2 shows the construction of the graphical solution*. The hyperbola through the experimental points is in this case calculated by using the analytical results from method (5) (8). The experimental points from Table VIII are represented by circles and the deviations are very small. The assymptotes $b = 6.246$ and $z = -.848$ are also indicated.

Between the results from (5)(8) and (8a) there is no practical difference. The agreement between the r value, calculated by the theoretical equation (5), and the experimentally determined r from (8a), is good. This is considered as a proof of the correctness of the theory. Also it is noted that the boundary of W_2C as determined by the independent lattice parameter method indicates almost the same composition.

---

* Note: The graphical results in Table IX are not obtained from this accurate construction.

Figure 2

X-Ray Intensity Ratio versus Composition WC + W_2C Alloys

The circles represent the experimental values of Table VIII. The hyperbola is computed by equation (6) using constants determined by equations (5) and (8).

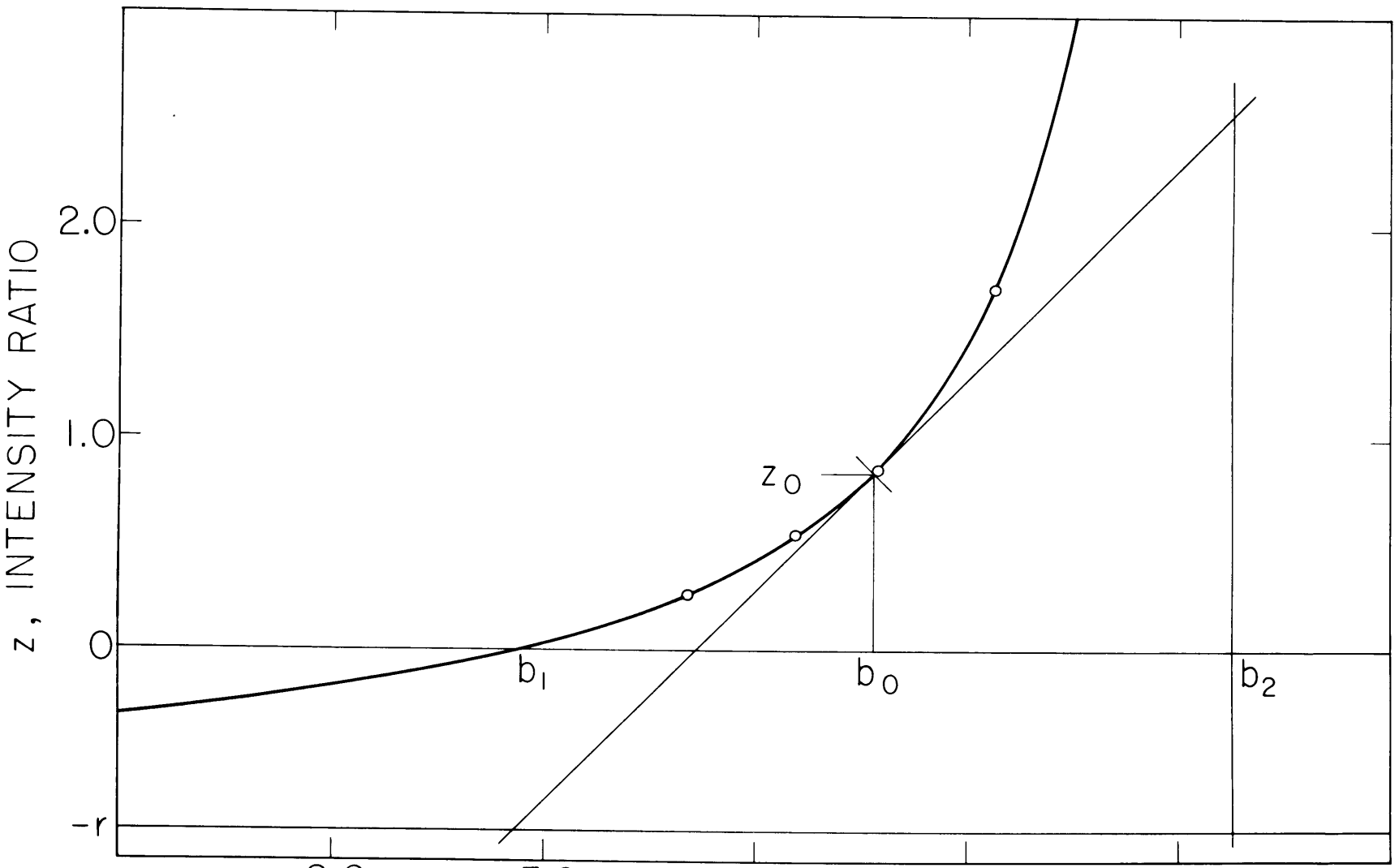
z, INTENSITY RATIO
2.0
1.0
0
-r
z_0
b_1
b_0
b_2
2.0
3.0
4.0
5.0
6.0
b, CARBON, PERCENT BY WEIGHT

FIGURE 2

6. Wolfram - Carbon Diagram

6.1 Diwolfram Carbide

The determinations of the composition range of W_2C by two independent methods indicate that this carbide possesses a defect lattice. If decimal indices are used in stoichiometric formula, the limiting compositions of W_2C can be written: $W_2C_{.79}$ and $W_2C_{.92}$. The latter can be considered as the most stable. From these formulae it can be seen that there is carbon deficiency in the W_2C lattice. Becker's[16] solution of the W_2C structure leads to a layer structure of the following fashion:

-C-W-W-C-W-W-C-

From the dimensions of the unit cell it is evident that there is no space for extra W atoms. The carbon deficiency could, however, be explained in two ways. The first possibility is that there is, on the average, more than 2 wolfram layers per 1 layer of carbon. Stacking faults of this type would cause two-dimensional reflections. General reflections (h,k,l) would diminish and the two-dimensionsal reflections (h,k) would appear with unsymmetrical line shape. The change of lattice constant "a" with carbon content would be negligible. Equations on page 12, however, show that "a" varies and more so than "c". Also no unsymmetry was noticed in the lines of the W_2C pattern. It is therefore felt that stacking faults are excluded. The second possibility, the incompletely filled carbon layers, seems more likely. This type of defect causes changes in the lattice constants.

The decimals in the above formulae give directly the fraction of positions occupied by carbon atoms. The stable range consists of from 8 to 21 percent unoccupied positions. It is easy to understand that more vacancies would cause the lattice to collapse, but more difficult to see why all positions cannot be occupied. Preliminary calculations have shown that lattice constants of $W_2C_{.92}$ give the atomic coordinates which Becker[16] measured, if diamond radius for carbon atoms is assumed. If more carbon would dissolve, the lattice constants increase to a value where carbon atoms no longer fill the interstities. The problem can be completely solved only by precision determination of the intensities of the W_2C lines. The intensities are functions of the z coordinates of the wolfram atoms, which uniquely would determine the radii of both carbon and wolfram atoms.

The high hardness of W_2C is explainable by means of the vacancy theory. Goldschmidt[27] has brought up this fact, but considers as possible only the stacking faults in W_2C containing an excess of carbon. The vacancy theory, as explained here would cause deformation of wolfram layers and simulate a structure somewhat similar to the diamond structure, where the carbon layers are puckered.

6.2 Monowolfram Carbide

For the composition range of WC there is no check available by the parameter method. The stoichiometric formula WC represents 50.00 atomic percent of carbon. The b_2 values in this experiment are high by .5 atomic percent. If this deviation is due to segregation it would mean that, in pulverizing the specimen, W_2C breaks into finer particles than WC. Otherwise

W_2C as the heavier phase would sink to the bottom layer of the spectrometer specimen, and the limit b_2 would move toward the lower carbon content. It seems more likely that each single particle consists of two phases.

Whether the high value of the WC limit is due to errors or of real significance, is difficult to judge from one series of experiments. However, the agreement at the W_2C limit is appreciably better than .5 atomic percent.

6.3 Wolfram-Carbon Diagram

The equilibrium diagram for wolfram carbon system has been worked out by Sykes[2]. Figure 3 represents this diagram modified by the results of this work. In case some changes have been made, the original boundaries by Sykes have been represented by dotted lines. The experimental points on which Sykes has based his diagram, are included in Figure 3. These points indicate that the temperatures of both eutectics are well fixed, whereas there is hardly any evidence to fix the homogeneity range of W_2C or WC. It appears as if the stoichiometric compositions have been adopted as such, even when a specimen of the stoichiometric composition after heating to 2700°C showed partial melting. Sykes made no attempt to continue the solubility limits of W_2C below 2400°C.

At the time Sykes constructed the wolfram carbide diagram, there was some evidence that the homogeneity range of W_2C at high temperatures extends rather far toward wolfram. The numerous analyses by Ruff and Wunsch[28] gave carbon contents in W_2C from 25.6 to 27.4 atomic percent. Later Horsting's[17] determinations of the wolfram rich boundary at 2200°C, indicated by triangles

Figure 3

Wolfram-Carbon Equilibrium Diagram

Open circles represent the phase boundaries as determined by the parametric method, Table V, solid circles by the intensity method, Table IX

Sykes'[2] measurements are indicated by squares and crosses, Horsting's[17] determinations by triangles.

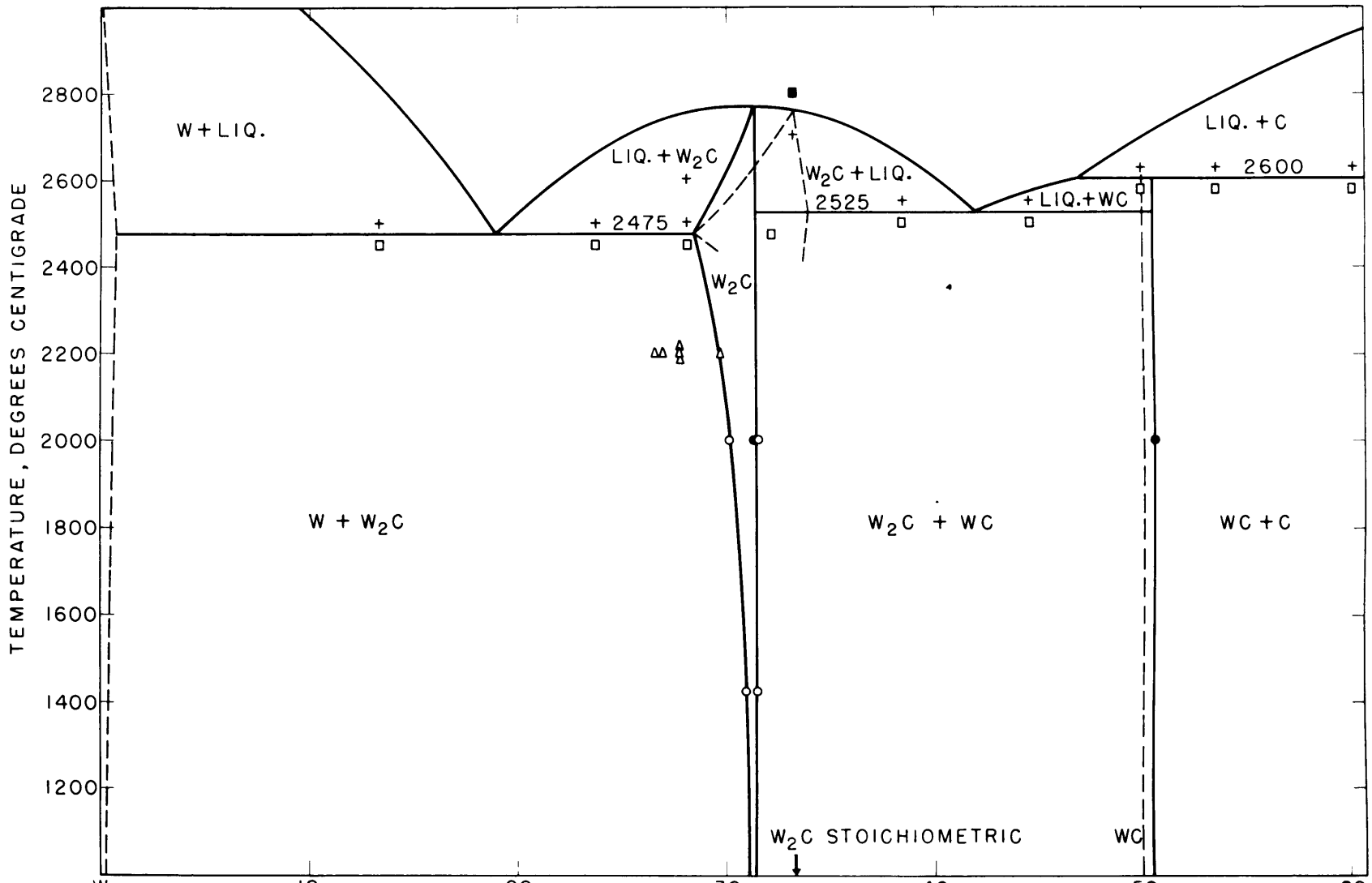
W + LIQ.
LIQ. + W2C
W2C + LIQ.
2525
+ 2475
+ 2600
+ LIQ. + WC
LIQ. + C
W2C
W + W2C
W2C + WC
WC + C
W2C STOICHIOMETRIC
WC
TEMPERATURE, DEGREES CENTIGRADE
2800
2600
2400
2200
2000
1800
1600
1400
1200
W
10
20
30
40
50
60
CARBON, ATOMIC PERCENT

FIGURE 3

in Figure 3, also show appreciable solubility. The scattering of Horsting's results however, is too high to be conclusive. The fact that wolfram carbide alloys of stoichiometric W_2C composition show extra wolfram carbide lines in x-ray patterns has been pointed out by Becker[16] and recently by Brownlee[1]. Brownlee however, interprets this fact as an indication of the unstability of W_2C.

Sykes diagram indicates no solubility for wolfram carbide. This carbide decomposes by peritectic reaction at 2600°C, a fact discovered already by Williams[13]. All attempts to determine the solubility limits of wolfram carbide have failed so far and therefore the simple formula WC has been generally accepted.

A deviation from the exact WC formula would offer an explanation of the high hardness of wolfram carbide. The results of this experiment indicate such a deviation, but it is too early to draw any final conclusions. The boundary can be checked by approaching the WC field from the opposite direction, that is from the WC + C field.

It is finally pointed out that the diagram established in Figure 3 does not disagree with any earlier work, especially concerning W_2C. The change of the WC field is only tentative.

7. Ternary Diagram Wolfram Cobalt Carbon

7.1 Sintering Experiments

To study the phase formation in wolfram-cobalt-carbon system, a series of specimens was sintered at 1400°C. This temperature was chosen because it is the common sintering temperature of the cemented carbides. This temperature is below all the temperatures of the invariant reactions in the adjoining binary systems except the cobalt-carbon eutectic. The sintering in solid state was considered desirable to avoid excess carburization or decarburization and evaporation of cobalt. At 1400°C, on the other hand, the solid state reactions proceed in a reasonable time.

The principal method of investigating the sintered specimens was x-ray diffraction by the Norelco recording spectrometer. Approximate determinations of the phase boundaries were made by the disappearing phase method.

The specimen preparation for microscopic examination encountered severe difficulties. The densification of the specimens was incomplete, if no liquid phase formation had occurred. This was so even in cases, where x-rays indicated complete formation of a phase. It also became evident later that all the ternary phases etched identically.

In this experiment two ternary phases, called here theta (θ) and kappa (K) were formed in addition to the well-known eta phase.

7.2 Eta Phase

This phase, which has been completely described by Westgren[29], showed a range of homogeneity from 7 to 20 percent of carbon and from 38 to 48 percent of cobalt. At 1400°C the eta phase was found to be in equilibrium with

monowolfram carbide, theta, wolfram, delta, beta and liquid. The boundaries toward beta and liquid were difficult to determine and appeared to be very temperature sensitive. The other boundaries are believed to be well fixed.

The homogeneity range of eta, as measured in this work, is considerably smaller than the one reported by Brownlee[1]. The two eta phases, assumed by Sandford and Trent[21], are the limiting compositions of eta saturated by cobalt and wolfram.

7.3 Theta Phase

The composition of theta phase corresponds to formula $Co_3W_6C_2$. It has cubic symmetry and its structure is closely related to the eta structure. The axial length of the face centered cubic lattice was measured as 11.25 A. The order of the diffraction lines was similar to those of eta, but the relative intensities were different. The characteristic x-ray patterns of eta and theta are given in Table X.

The composition range of the theta phase was narrow, about 2 percent. At 1400°C theta was in equilibrium with monowolfram carbide, kappa, wolfram and eta. There was a well defined two phase field between eta and theta. A series of specimens, which had their compositions in this field, showed a gradual transition of the relative intensities from the eta pattern to the theta pattern, without any change in the lattice constants. Figure 4 shows the x-ray pattern of an alloy in the middle of the two phase field eta + theta.

There is no mention in the literature of a phase of composition $Co_3W_6C_2$. However, the phase Co_2W_4C, proposed by Kisloykova[20] has the same cobalt-wolfram ratio but 4 percent less carbon.

Table X

X-Ray Patterns of Eta, Theta, and Kappa Phases

Planar Spacings (d) and Relative Intensities (I) of Reflections

Eta Phase

h k l	d	I
400	2.740	.24
331	2.514	.36
420	2.450	.00
422	2.237	.65
511, 333	2.109	1.00
440	1.937	.50

Theta Phase

h k l	d	I
400	2.813	.09
331	2.581	.41
420	2.516	.00
422	2.296	.51
511, 333	2.165	1.00
440	1.989	.44

Table X (Continued)

Kappa Phase

h k l	d	I
20.0, 10.2	2.299	.10
20.1	3.118	.14
11.2	2.778	.00
00.3	2.620	.00
20.2, 12.0	2.568	.75
10.3, 21.1	2.447	.80
30.0	2.268	.36
30.1, 11.3	2.179	1.00
21.2	2.152	1.00
20.3	2.074	.60
30.2, 22.0, 00.4	1.962	.40
22.1	1.904	.00
31.0, 10.4	1.886	.10
31.1, 21.3	1.836	.10
22.2, 11.4	1.757	.15
30.3	1.714	.00
40.0, 31.2, 20.4	1.702	.35
40.1	1.664	.00
22.3, 00.5	1.570	.00
40.2, 32.0, 21.4	1.560	.15
32.1, 31.3, 10.5	1.530	.00
41.0, 30.4	1.484	.00
41.1, 11.5	1.459	—
32.2	1.451	.00
40.3, 20.5	1.427	.23
41.2, 22.4	1.389	.00
50.0, 31.4	1.361	.25
50.1, 32.3, 21.5	1.340	.56
33.0, 00.6	1.308	.35
41.3, 33.1, 30.5	1.291	.35
50.2, 42.0, 40.2, 10.6	1.285	.40

Figure 4

X-Ray Spectrometer Pattern of Eta and Theta Phases

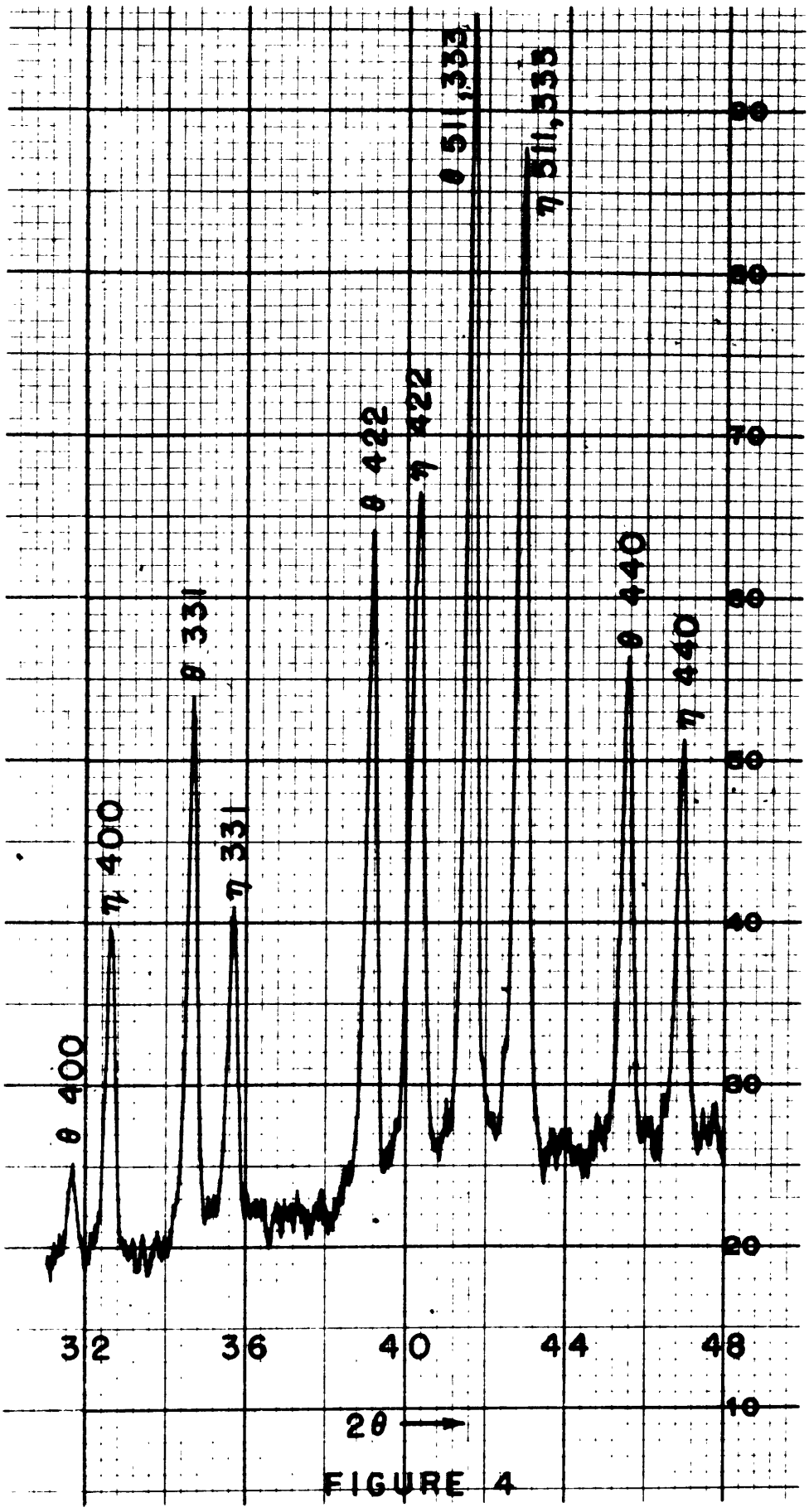
θ 400
η 400
θ 331
η 331
θ 422
η 422
θ 511, 333
η 511, 333
θ 440
η 440
32
36
40
44
48
2θ
90
80
70
60
50
40
30
20
10

FIGURE 4

Figure 5

X-Ray Spectrometer Pattern of Kappa Phase

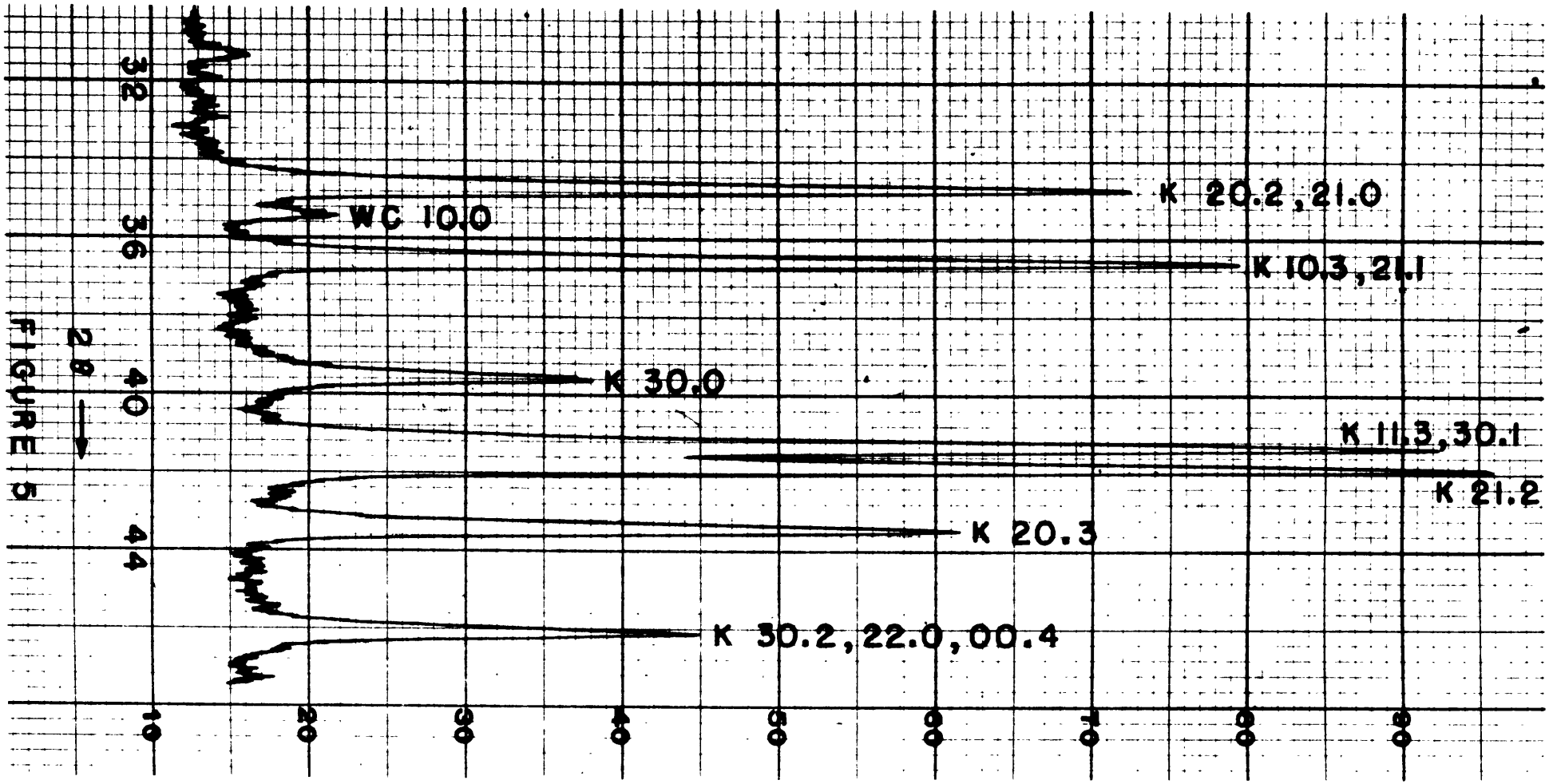
K 20.2, 21.0
WC 10.0
K 10.3, 21.1
K 30.0
K 11.3, 30.1
K 21.2
K 20.3
K 30.2, 22.0, 00.4
32
36
40
44
2θ
10
20
30
40
50
60
70
80
90

FIGURE 5

7.4 Kappa Phase

Kappa phase correspond to the formula $Co_3W_{10}C_4$. Its range of homogeneity was very narrow, less than 1 percent. The lattice was found to be hexagonal and the lattice constants a and c were both equal and measured as 7.848 A. The diffraction lines of the kappa phase are given in Table X and a typical x-ray pattern is reproduced in Figure 5. The kappa phase was found to be in equilibrium at 1400°C with mono and divolfram carbides, wolfram and theta.*

7.5 Isothermal Section at 1400°C

By combining the results of this experiment with the 1400°C isothermal lines from the adjoining binary diagrams it was possible to construct an isothermal section of wolfram-cobalt-carbon diagram. This 1400°C isothermal section is illustrated in Figure 6. The equilibria in the wolfram rich part of the section have been described in connection with the ternary phases.

Of special interest is the two-phase field, WC + liquid, which extends across the isothermal section. After cooling to room temperature specimens in this field showed a two phase structure, beta + WC. Occasionally, depending on the carbon centent, eta or graphite was found in addition. The two phase field beta + WC was very narrow, about 1 percent.

The WC phase seems to have a very small solubility for cobalt. All attempts to measure any changes in the lattice constant of WC failed. Very contradictory solubilities have been reported in the literature. The

---

* Note: The theta and kappa phases were readily formed in the iron-wolfram-carbon and in the nickel-wolfram-carbon systems with the same compositions and lattices.

Figure 6

1400°C Isothermal Section of W-Co-C Equilibrium Diagram.

Point A represents the composition of the cemented carbides of 18 weight percent cobalt content. The dotted lines B-C and Co-WC correspond to the vertical sections of Figures 9 and 11.

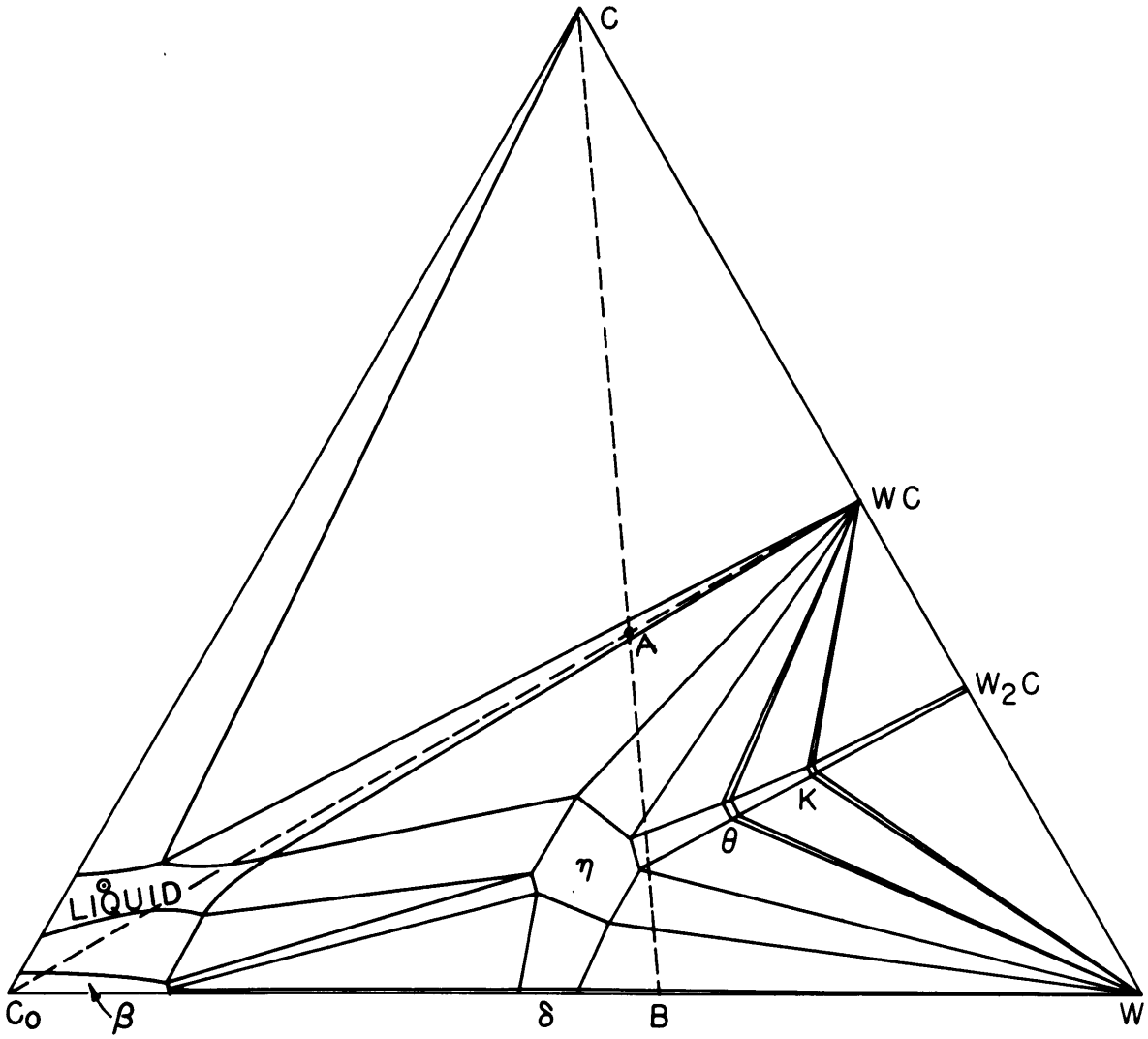

FIGURE 6

most dependable seem to be the magnetic measurements made at Krupp-Widia Works[24], which indicate about .2 percent cobalt in solution in WC at 1400°C.

The boundaries of the liquid phase are known only approximately. The phase extends from the eutectic of the cobalt-carbon binary toward the eta phase.

7.6 Thermal Analyses

The invariant temperatures of the reactions leading to three phase equilibria beta + WC + graphite and beta + eta + WC were determined by thermal analysis. The measurements were made by a modified inverse-rate technique, which is described in Appendix VI. The cooling curves are reproduced in Figure 7. Alloys in equilibrium with graphite showed a thermal arrest at 1298°C, as indicated by the curves for specimen E, which had a composition of 27.3 percent of wolfram and cobalt, and 45.5 percent of carbon. The specimen D, which has 25 percent of carbon and equal amounts of wolfram and cobalt, had a thermal arrest at 1357°C. This alloy was in equilibrium with eta.

7.7 High Temperature Experiments

To establish the reactions which lead to the formation of the eta, theta and kappa phases, a series of alloys which consisted of one or two of these phases was heated to temperatures of 1700°C and 1880°C. The specimens were first prepared by sintering at 1400°C. After rapid cooling from 1700°C, the theta and kappa phases showed no changes but the specimens containing eta indicated increasing amounts of theta. The eta specimens were melted and full of large gas holes, apparently due to evaporation of cobalt.

Figure 7

Cooling Curves of Three Phase Alloys Beta-Graphite-WC and Beta-Eta-WC.

Composition of specimen E:

27.3 percent of wolfram, 27.3 percent of cobalt and 45.5 percent of carbon

Composition of specimen D:

37.5 percent of wolfram, 37.5 percent of cobalt and 25.0 percent of carbon

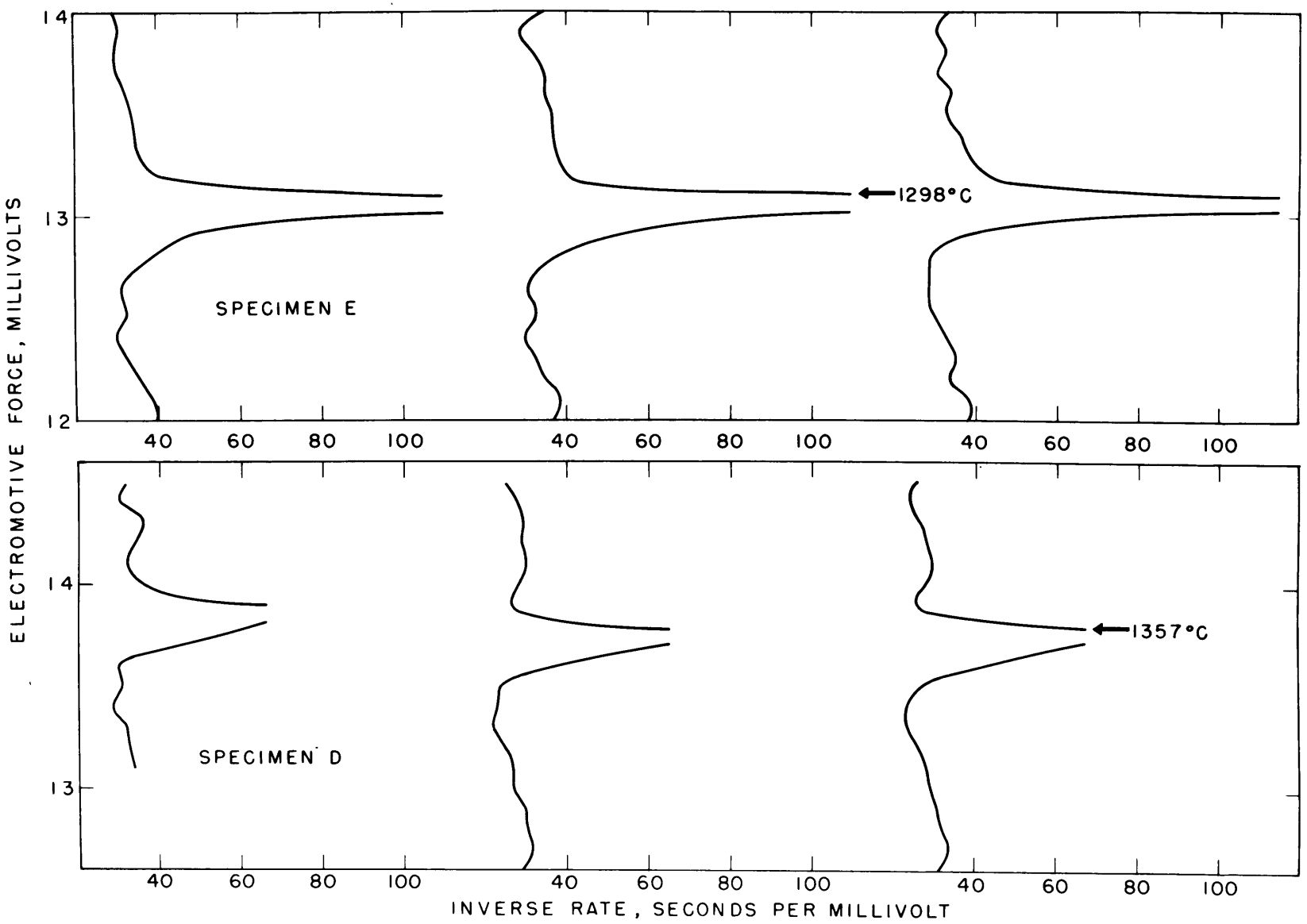
ELECTROMOTIVE FORCE, MILLIVOLTS
14
13
12
SPECIMEN E
1298°C
40
60
80
100
14
13
SPECIMEN D
1357°C
INVERSE RATE, SECONDS PER MILLIVOLT

FIGURE 7

After heating to 1880°C both theta and kappa showed decomposition. A specimen, originally pure theta, recorded x-ray lines of kappa and wolfram in addition, whereas a specimen of kappa composition showed strong lines of theta, kappa and W_2C and weaker lines of wolfram.

These observations suggest the following peritectic reactions:

$$\theta = \text{Liquid} + K + W$$

$$K = \text{Liquid} + W_2C + W$$

In the case of θ the cobalt rich liquid probably decomposed by evaporation. Traces of W_2C found in the theta specimen support this assumption. The liquid from the kappa decomposition probably solidified under non-equilibrium conditions into theta and kappa. Because the amount of the liquid, as indicated by the intensities of the theta lines, was large, the composition of this liquid apparently was not far from the kappa composition. The small amounts of wolfram found were in accordance with this view.

8. Tentative Metastable Diagram Wolfram-Cobalt-Carbon

The experimental evidence described enables one to construct a tentative model of the wolfram-cobalt-carbon diagram. It will be shown later that this diagram is of metastable nature.

The model is illustrated in Figure 8, which shows the basal projection of the lines of two-fold saturation. The notation used refers to this figure. The simplifications made in designing the model are:

1. All the allotropic transformations which occur in the components wolfram, graphite, cobalt and probably in the phase W_2C are omitted.
2. The complications caused by the gamma phase Co_3W have not been considered.
3. The vapor phase of cobalt is not included.

It is believed that these simplifications are justified, because the allotropic phase transformations as well as the gamma formation occur at temperatures which are outside of the range of the primary interest.

The general appearance of the diagram is determined by the very high melting points of carbon and wolfram. The liquidus surface slopes sharply toward the cobalt corner. A valley extends from the eutectics on the wolfram-carbon binary across the diagram. This valley of low melting is defined by the lines of two-fold saturation.

The three lines of two-fold saturation, liquid-WC-graphite, liquid-WC-W_2C and liquid-W_2C-W, cannot meet one another. Because of this fact all ternary eutectic reactions are excluded above 1690°C, where the first line of two-fold saturation is available from the cobalt-wolfram system.

Figure 8

Metastable Equilibrium Diagram Wolfram-Cobalt-Carbon.
Representation by Basal Projection.

P_1 Liquid + W_2C + W = K

T_1 Liquid + W_2C = K + WC

P_2 Liquid + K + W = Θ

T_2 Liquid + K = Θ + WC

P_3 Liquid + Θ + W = η

T_3 Liquid + Θ = η + WC

T_4 Liquid + W = η + δ

T_5 Liquid + δ = β + η

T_6 Liquid + η = WC + β

T_o Liquid = WC + β + graphite

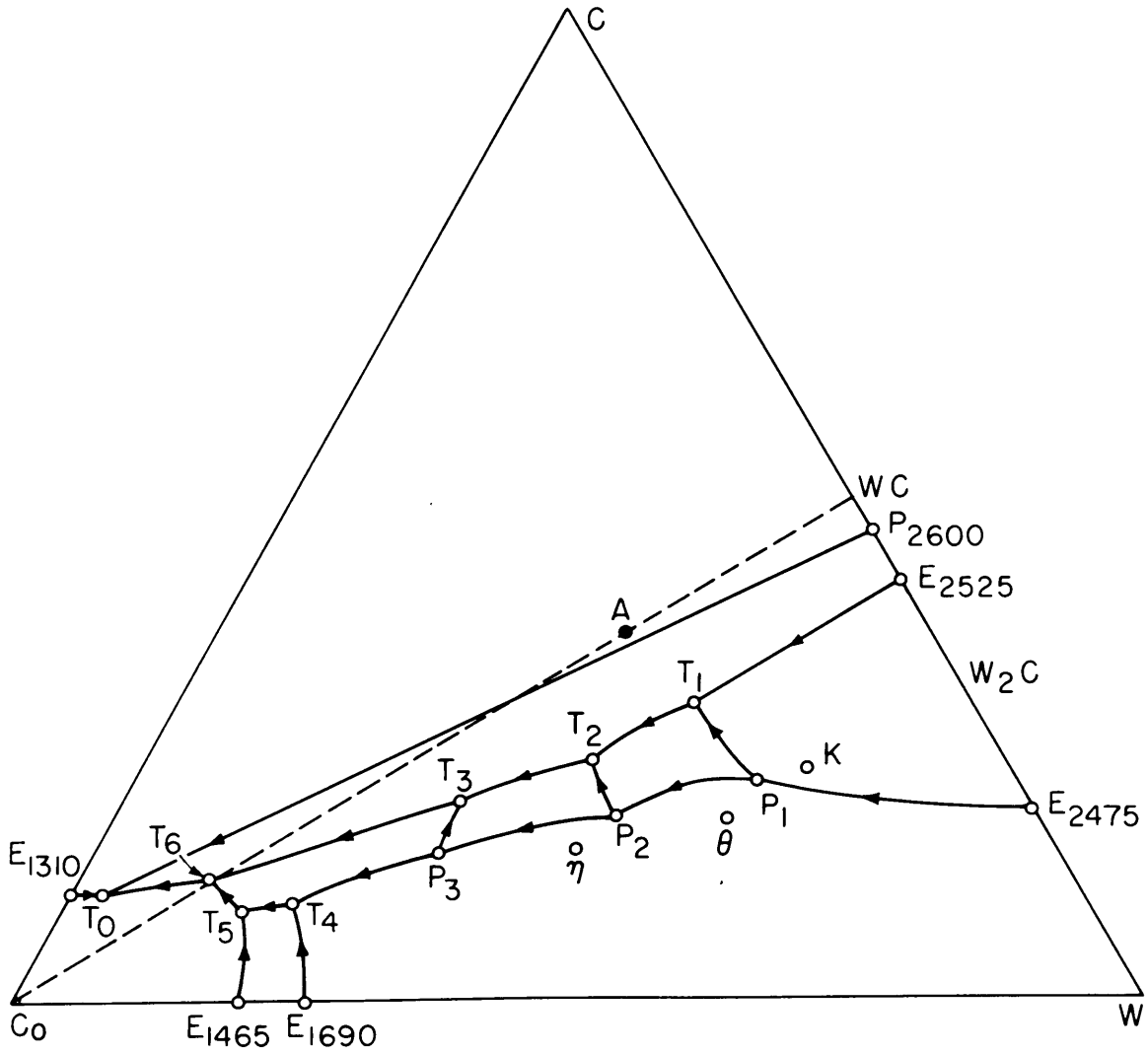
C
WC
P2600
E2525
A
W2C
T1
T2
T3
K
P1
E2475
T6
E1310
P2
θ
P3
η
T0
T5
T4
Co
E1465
E1690
W

FIGURE 8

The line of two-fold saturation, which extends from the WC peritectic at 2600°C, represents the liquid-WC-carbon equilibrium. This line has to encounter the two-fold saturation line from the cobalt-carbon eutectic to generate the three phase equilibrium beta-WC-graphite.

The invariant temperature of this four phase equilibrium, liquid-beta-WC-graphite, was measured as 1298°C, which was the lowest reaction temperature found. The average temperature of the lowest melting in sintering commercial two-phase alloys, beta + WC, seems to be about 1320°C[21]. The invariant reaction at 1298°C therefore has to be a eutectic reaction:

$$\text{Liquid} = \beta + WC + C$$

For this reaction a third line of two-fold saturation beta - WC has to be supplied over the section cobalt - WC. This link in the chain of reactions will be completed later.

The kappa phase was found to be stable at temperatures above 1690°C. Therefore kappa phase can only be formed by a peritectic reaction. Because no WC was found in the decomposed kappa, the reaction must be

$$\text{Liquid} + W + W_2C = K$$

The composition of the liquid, indicated by the letter P_1, is not far from the kappa composition. The reaction temperature is near 1880°C because of the three kappa specimens heated to 1880°C, two decomposed and one did not. Since the accuracy of the temperature measurement in this range is about $\pm$ 15°C, this means that the invariant temperature is between 1865°C and 1895°C. The reaction provides the two phase equilibria K + W_2C and K + W, which were found at 1400°C.

To obtain the kappa - WC equilibrium, also found, a ternary transition

$$\text{Liquid} + W_2C = K + WC$$

has to occur at somewhat lower temperature T_1, where the lines of two-fold saturation liquid - WC - W_2C and liquid-W_2C - K come together.

The formation of the theta phase is similar to the kappa reaction and in accordance with the experiments the peritectic reaction is:

$$\text{Liquid} + K + W = \theta$$

The reaction temperature P_2 is in the neighborhood of 1700°C, but not known accurately. This reaction furnishes the experimentally found two-phase fields θ + K and θ + W. The ternary transition

$$\text{Liquid} + K = \theta + WC$$

caused by intersection of the lines liquid - kappa-WC and liquid - kappa - theta provides the two phase field theta + WC. This reaction temperature T_2 has to be lower than P_2.

There is not much experimental support to the nature of the eta reaction. The various attempts made, were upset by the evaporation of cobalt, It is believed that the temperature of the invariant reaction of the eta formation is about 1600°C. From the nature of the diagram it can be concluded that the peritectic reaction Liquid + θ + W = η is the only possibility. The three lines of two-fold saturation, available at this stage, are of such nature that they cannot meet.

The reaction Liquid + θ + W = η would give the two phase fields η + θ and η + W. The double saturated liquids, liquid-theta-eta and liquid-theta- WC, react at lower remperature supplying the field η + WC.

The experimentally verified eta-delta field is a product of ternary transition Liquid + W = $\eta + \delta$, which occurs when the lines of two-fold saturation Liquid-eta-wolfram and Liquid-delta-wolfram come together.

The eta-beta equilibrium, which exists at 1400°C and below, is formed by a ternary transition: Liquid + $\delta = \eta + \beta$. This reaction consumes the last two-fold saturation line coming from the binary eutectic at 1465°C of the cobalt-wolfram system.

The two double saturated liquids, liquid-eta-beta and liquid-eta-WC, react at 1357°C in a ternary transition reaction; Liquid + $\eta = \beta$ + WC, forming the important two phase equilibrium beta - WC. This reaction also supplies the missing link to complete the ternary eutectic reaction at 1298°C, mentioned on page 49.

Not much has been said as to the compositions of the reacting phases. This is especially true with the compositions of the saturated liquids. The solid phase compositions are, in general, well fixed. It has been revealed in this study that the homogeneity ranges of all participating phases are very narrow. The only exception is the eta phase.

It is possible to locate the ternary eutectic to within a few percent by pure speculation. The ternary eutectic temperature was measured as 1298°C. The binary eutectic reaction; Liquid = β + C has been reported between 1300°C and 1315°C. The difference is very small, as a matter of fact within the experimental errors. It is unlikely that the ternary eutectic composition would be far from the cobalt-carbon binary. But on the other hand, there is cumulative evidence that the maximum solubility of WC in cobalt is about 10 percent. Yet the eutectic point has to be within

the three phase field corner and not far from the section Co-WC because toward the carbon corner the liquidus surface is almost vertical.

One point of extreme practical importance is the composition of the liquid phase in the reaction: Liquid + η = β + WC. Figure 9 represents a vertical section through the carbon corner of the diagram for constant wolfram - cobalt ratio of 57/43. This is a section which includes cemented carbides of 18 weight percent cobalt content. An alloy of this composition, which at low temperatures would have a two phase beta + WC structure, is represented by line A. It is evident that the extension of the invariant plane at 1357°C will determine whether or not eta phase is formed during heating or cooling of the specimens. The question is important because it will form the basis of understanding the sintering mechanism of the cemented carbides.

The reactions occurring during cooling from the sintering temperature can be followed by Figure 10. The common sintering temperature is about 1400°C. The specimen at this temperature consists of solid WC and liquid. During cooling WC precipitates and composition of the liquid follows the surface of one-fold saturation until the line $T_6 - T_o$ is encountered. During further cooling WC and beta precipitate simultaneously. The composition of the precipitating beta follows the curve d - e. When the line WC - β" intersects the vertical A, all liquid has been consumed and solidification is complete. Depending on the cooling rate, various amounts of WC will precipitate out of the beta solid solution during subsequent cooling to room temperature.

Figure 9

Vertical Section through Carbon Corner of Metastable W-Co-C Diagram

Wolfram - Cobalt ratio = 57/43

The dotted line A corresponds to the composition of the cemented carbide of 18 weight percent cobalt content.

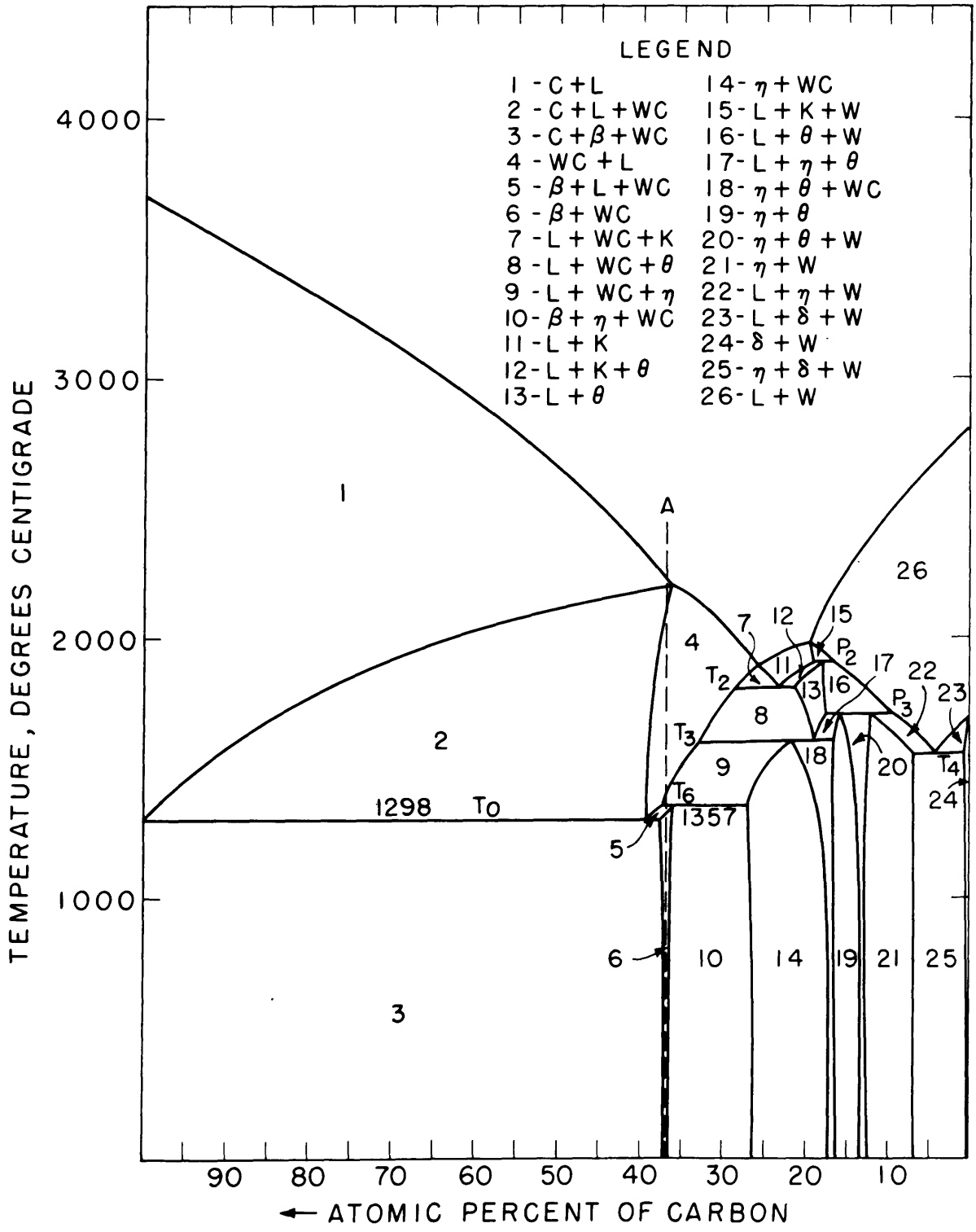
LEGEND
1 - C + L
2 - C + L + WC
3 - C + β + WC
4 - WC + L
5 - β + L + WC
6 - β + WC
7 - L + WC + K
8 - L + WC + θ
9 - L + WC + η
10 - β + η + WC
11 - L + K
12 - L + K + θ
13 - L + θ
14 - η + WC
15 - L + K + W
16 - L + θ + W
17 - L + η + θ
18 - η + θ + WC
19 - η + θ
20 - η + θ + W
21 - η + W
22 - L + η + W
23 - L + δ + W
24 - δ + W
25 - η + δ + W
26 - L + W
TEMPERATURE, DEGREES CENTIGRADE
4000
3000
2000
1000
A
1298 To
1357
T2
T3
T4
T6
P2
P3
90 80 70 60 50 40 30 20 10
← ATOMIC PERCENT OF CARBON

FIGURE 9

Figure 10

Perspective Illustration of Solidification of
Cobalt Cemented Wolfram Carbides

The composition of the alloy is given by vertical line A.
Points D and E indicate the approximate compositions of
the thermal analysis specimens, page 45.

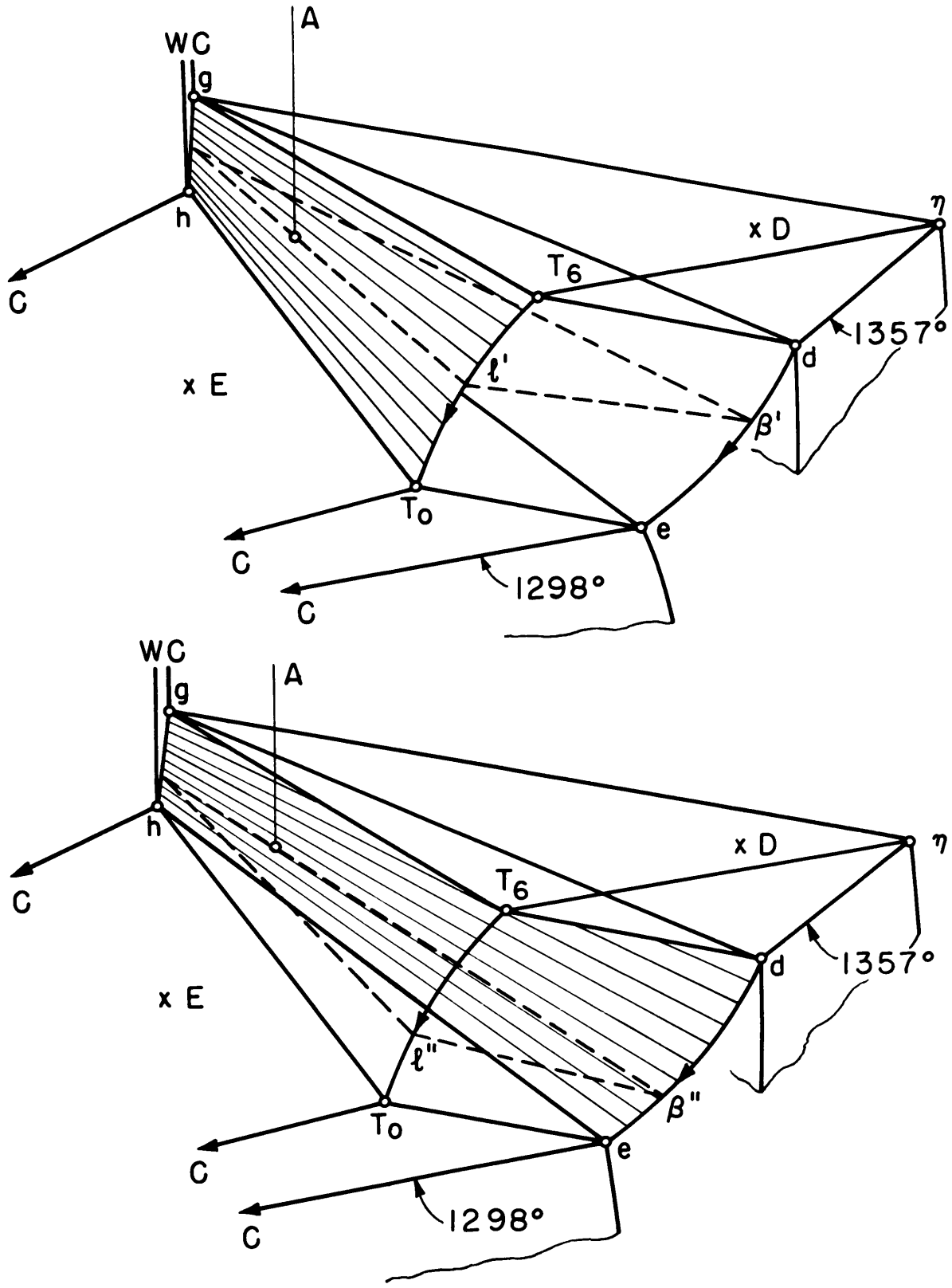
WC
g
A
h
C
x E
x D
η
T6
1357°
d
ℓ'
β'
To
e
C
C
1298°
WC
g
A
h
C
x D
η
T6
1357°
d
x E
ℓ"
β"
To
e
C
C
1298°

FIGURE 10

If the invariant plane g-T_6-d-η extends completely over the two phase field WC + beta, the two-fold precipitation will be WC + eta until the invariant temperature is reached.

The vertical section cobalt-WC is illustrated in Figure 11. Because it is not known whether or not the 1357°C invariant plane extends over the two phase field beta + WC, a compromise has been made by drawing a special case represented by point at 1357°C. If the carbon content of the saturated liquid at 1357°C is higher than indicated, two three phase fields and one two phase field will be generated from the point at 1357°C. In the opposite case the four phase equilibrium will disappear.

Figure 11

Vertical Section Cobalt-Wolfram-Carbide

Because experimental data is lacking, a special case is illustrated.

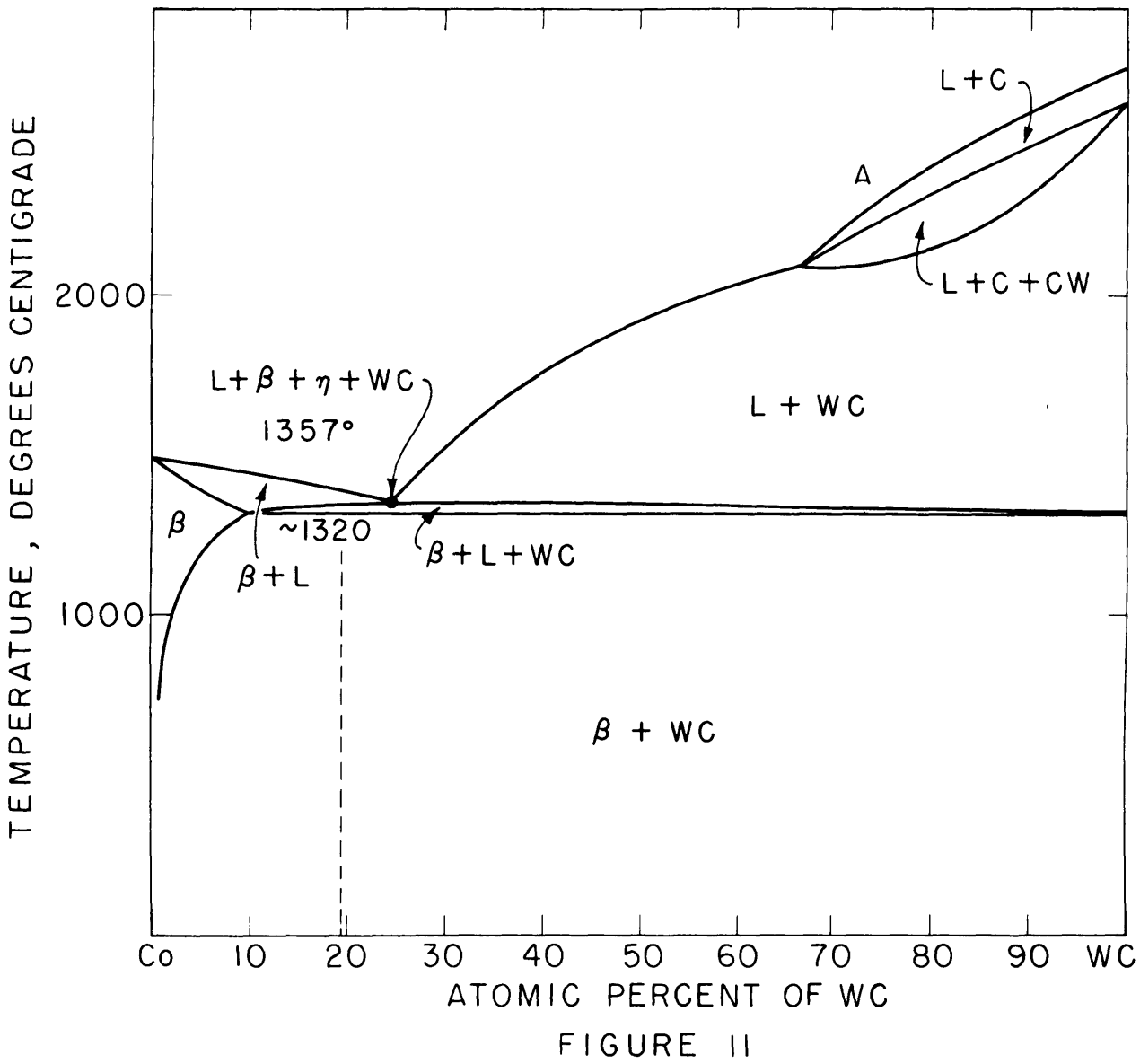
TEMPERATURE, DEGREES CENTIGRADE
2000
1000
L+C
A
L+C+CW
L+β+η+WC
1357°
L + WC
β
~1320
β+L
β+L+WC
β + WC
Co
10
20
30
40
50
60
70
80
90
WC
ATOMIC PERCENT OF WC

FIGURE 11

9. Instability of Carbides

The instability of eta phase has been reported by Takeda[19] in the iron-wolfram-carbon system. The basis of Takeda's hypothesis seems to be a photomicrograph of an annealed eta grain, which according to Takeda, shows a rim of WC formed by decomposition of eta. However, it is believed here that the rim was nothing but eta, from which a heavy layer of etching stain has chipped off. If a more careful etching technique would have been applied, no such rim probably would have been visible.

Takeda's instability hypothesis was accepted by Westgren[18]. To verify it Westgren annealed a specimen of composition Ni_3W_3C for ten days at 1000°C and the result was WC. It is believed here that carburization took place in this experiment.

It will be shown by the following experiment that the eta phase is a stable phase.

A specimen of composition 81.0 percent cobalt, 9.0 percent wolfram and 10.0 percent carbon was heated to 1500°C in an alundum crucible by induction. At 1500°C the alloy was expected to consist of liquid phase only. The specimen was than furnace cooled. A section through the solidified specimen showed two types of structures. The surface layer, shown in Figure 12a, consists of primary beta surrounded by a fine structure of beta and WC. The center of the specimen, shown in Figure 12b, also shows primary beta but now surrounded by eta-beta eutectic and numerous graphite flakes.

Figure 12

Microstructure of 9W-81Co-10C Alloy. 250X.

Etched by Alkaline $K_3 Fe(CN)_6$

a) Cross section near surface: Primary beta and WC + beta.

b) Cross section in core: Primary beta, eta + beta and graphite. Some indication of the mottled structure.

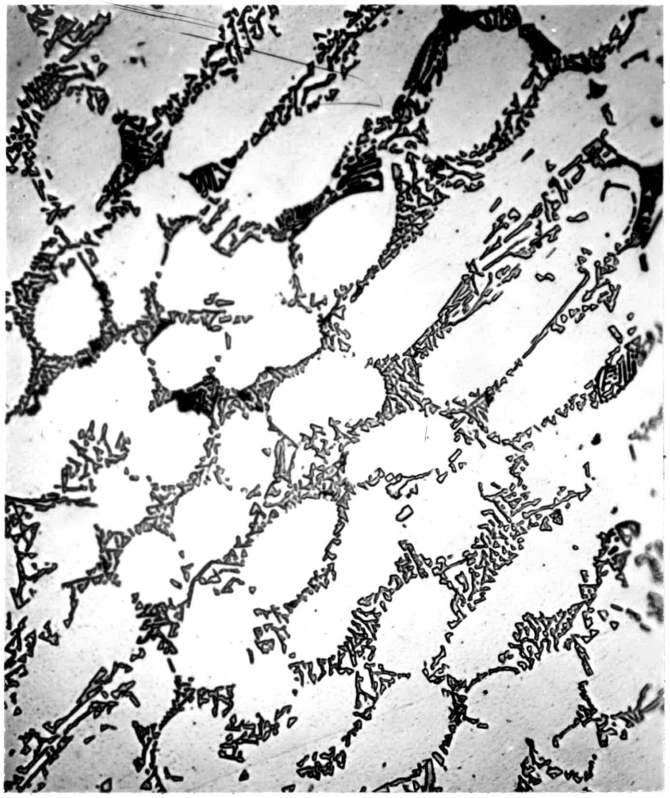

FIGURE 12 (a)

FIGURE 12 (b)

The condition in the furnace was only slightly carburizing, if at all. The alundum crucible was enclosed in a graphite crucible, which was completely packed in norblack.

The cooling rate on the surface of the specimen is expected to be faster than inside. The surface structure is in accordance with the metastable diagram. The cobalt corner of this diagram is represented in Figure 13, to which the following discussion is referred.

During the cooling from the liquid state the precipitation of beta starts when the surface of one-fold saturation, a - E_{1465} - T_5 - T_6 - T_o - E_{1310} has been reached. The composition of the liquid follows this surface away from the cobalt corner until the line T_6 - T_o has been encountered. The composition of the precipitating beta has moved on the surface a-b-c-d-e-f. During subsequent cooling simultaneous precipitation of WC and beta takes place. The composition of the precipitating beta at this stage is given by the line d-e. The composition of the specimen is such that all liquid is consumed before the eutectic temperature 1298°C has been reached.

The structure of the specimen core, apparently cooled slower, cannot be explained by means of the metastable diagram, which has no eta-graphite equilibrium. Apparently the core has approached true equilibrium conditions more closely and thus the combination cobalt-eta-graphite is the stable one. It will be noted that the composition of the specimen was not changed. The free graphite amounts to the difference between the carbon contents of WC, and eta.

Figure 13

Perspective Illustration of Cobalt Corner of Metastable W-Co-C Diagram.

a is the melting point of cobalt.
The solidus surface is a-b-c-d-e-f.
The liquidus surface a-E_{1465}-T_5-T_6-T_o-E_{1310}

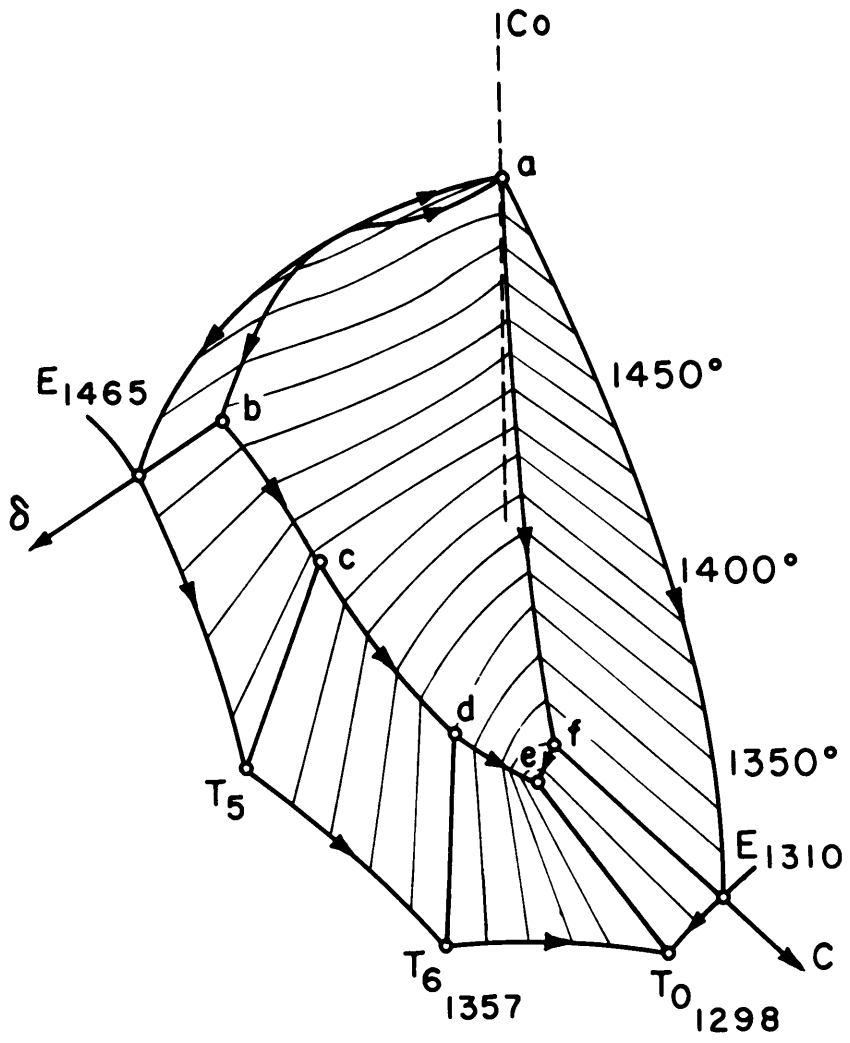

FIGURE 13

10. Tentative Model of Stable Diagram Wolfram-Cobalt-Carbon

A stable system may be developed from the metastable by omitting the ternary transition at 1357°C. Above 1400°C the stable and the metastable diagrams are of the same fashion. Below 1400°C there are three lines of two-fold saturation,

a. Liquid-graphite-WC

b. Liquid-eta-WC

c. Liquid-eta-beta

In the metastable system the lines b and c come together causing reaction:

$$\text{Liquid} + \eta = \beta + \text{WC}$$

In the stable system the lines a and b intersect and ternary transition:

$$\text{Liquid} + \text{WC} = \eta + \text{C}$$

produces the eta-graphite equilibrium.

The double saturated liquids; liquid-graphite-eta, liquid-eta-beta, and liquid-beta-graphite react at a lower temperature:

$$\text{Liquid} = \beta + \eta + \text{C}$$

to produce the three phase field beta-eta-graphite*

A model of the stable equilibrium diagram wolfram-cobalt-carbon is illustrated in Figure 14. The difference between the stable and metastable diagrams is best seen by means of isothermal sections at about 1200°C, Figures 15 and 16.

---

*Note: The temperature of the above eutectic reaction was not revealed by the thermal analyses described on page 45. Apparently the thermocouple protecting tube conducted efficient heat from the center of the specimen, which indicated no eta phase. It is believed that the temperature of the eutectic reaction in the stable system is lower than in the metastable system.

Figure 14

Stable Equilibrium Diagram W-Co-C. Representation by Basal Projection

The reactions P_1 - T_5 are the same as in Figure 8.

T_7 Liquid + WC = η + graphite

T_{o_s} Liquid = β + η + graphite

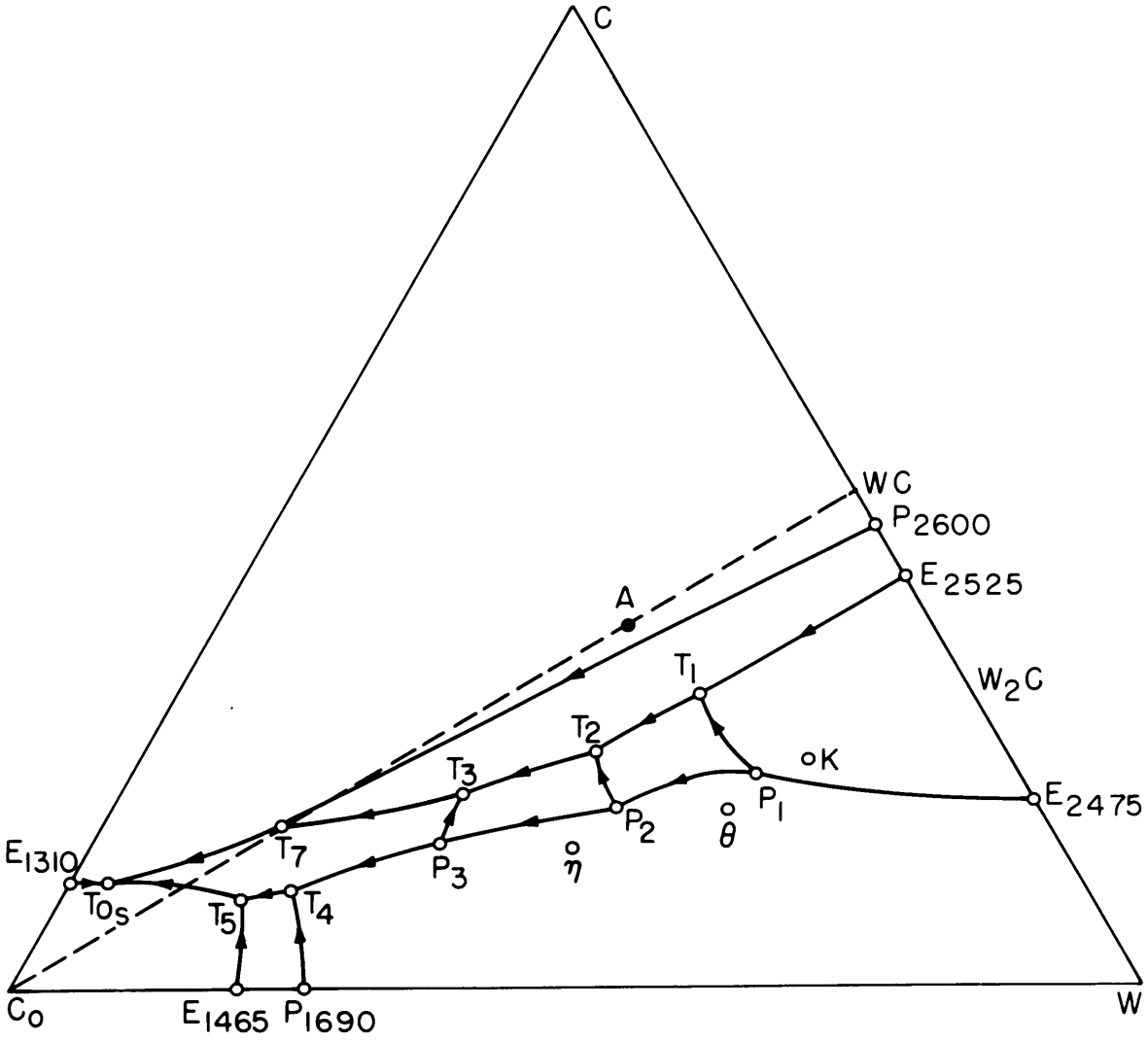
C
WC
P2600
E2525
A
T1
W2C
T2
T3
K
E2475
P1
P2
θ
E1310
T7
P3
η
T0s
T5
T4
C0
E1465
P1690
W

FIGURE 14

Figure 15

1200°C. Isothermal Section of Stable Diagram W-Co-C

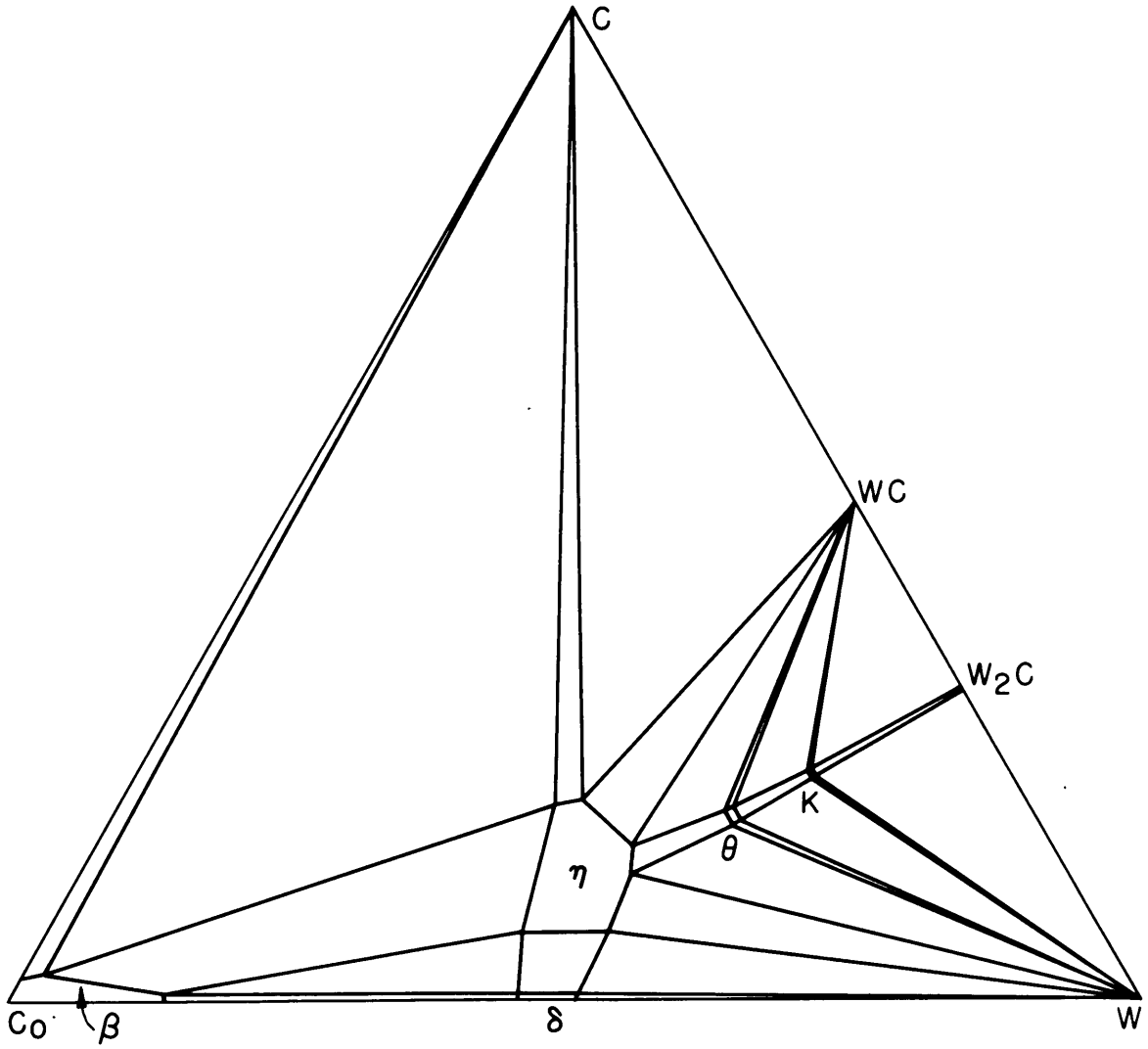

FIGURE 15

Figure 16

1200°C. Isothermal Section of Metastable Diagram W-Co-C.

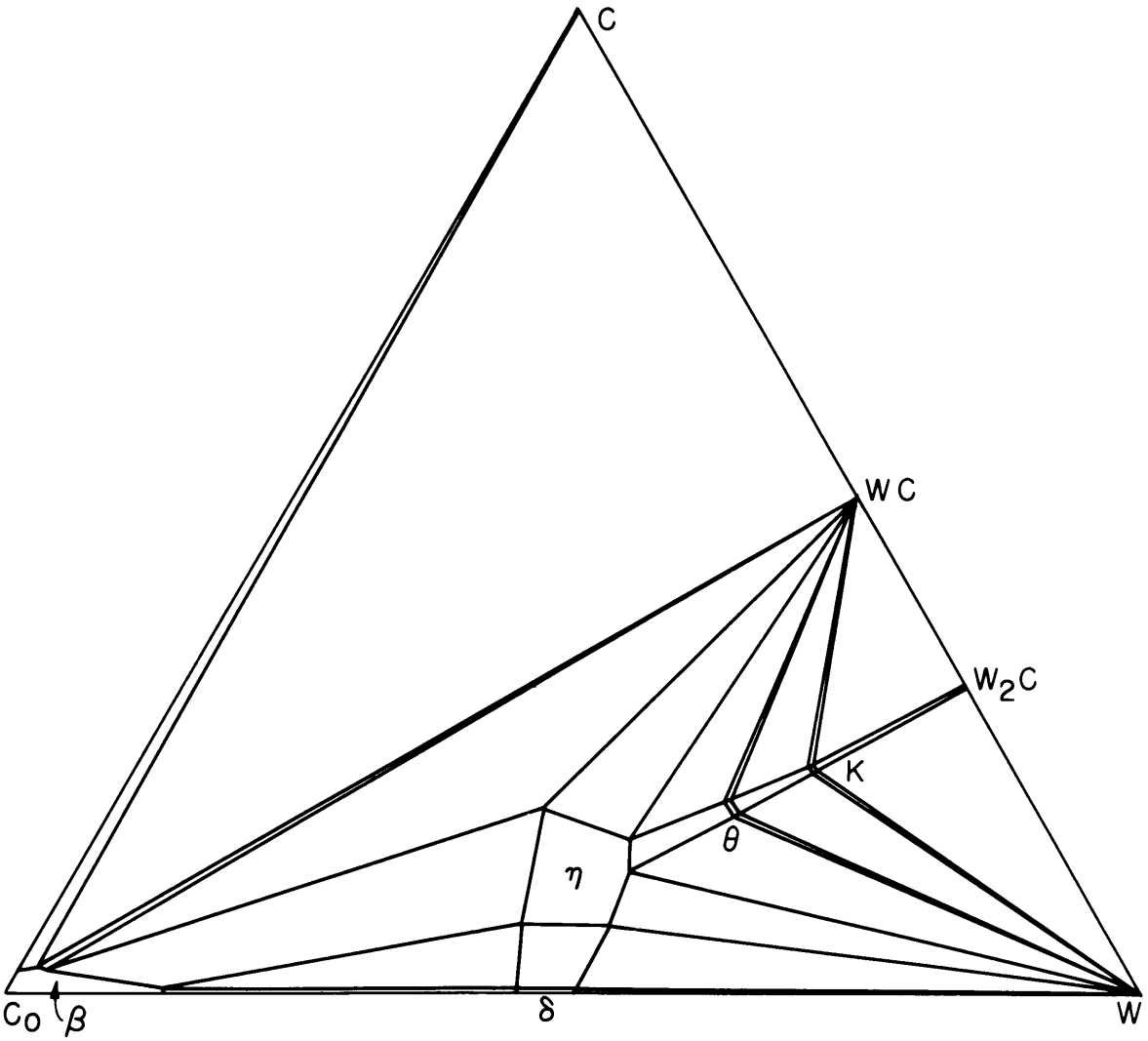

FIGURE 16

The characteristic feature of the metastable diagram is the two phase field beta - WC, which extends across the diagram. The cemented carbides should have this structure. In the stable system this important two phase equilibrium is destroyed. From the viewpoint of technical applications it is clear that the stable equilibrium is most undesirable. Therefore slow cooling rates from the sintering temperatures have to be avoided.

11. Discussion of the Results and Conclusions

The measurements done in this study can be divided into two categories depending on the accuracy applied. Into the first class where precision was aimed, belong the lattice parameter and intensity measurements in the wolfram-carbon system. The second group is of surveying nature and consists of the experiments on the ternary diagram.

a. The lattice constants of mono and diwolfram carbides were determined by precision methods. The scatter of the values is mainly caused by the temperature variations from sample to another, a fact unfortunately discovered too late. The high precision in measurements and calculations is therefore not completely justified, although the constants represent the precision obtainable without controlling the temperature of the specimen during the exposure. Because of the accidental nature of the temperature errors it is believed that the results are much improved by the least square technique applied.

b. The solubility limit determinations in the wolfram-carbon system by the lattice parameter and the intensity methods show a good agreement. The absolute compositions of the boundaries depend on the chemical analyses, but also here the scatter in the analytical carbon determinations has been smoothened by the least square method and independent series of specimens have been used for both methods.

c. The carbon deficiency in diwolfram carbide is not explainable by errors in chemical analyses, because the monowolfram carbide shows too high carbon content, and both determinations are based on the same analyses.

It would be impossible to carburize monowolfram carbide and decarburize diwolfram carbide at similar conditions. The opposite would be more likely.

Whether the high carbon content of monowolfram carbide found, is of real significance or due to errors is too early to decide. Errors by segregation are possible only if diwolfram carbide breaks into finer particles than monowolfram in the process of specimen preparation.

d. The results by the new intensity method agree with the values by the lattice parameter method. Also the theoretical and experimental constants show better agreement than would be expected considering the small number of specimens used. The few quantitative determinations done in connection with the segregation experiments indicate that the method is useful at its present state although further theoretical study of the segregation phenomenon is both desirable and promising.

The method is applicable to ternary systems but so far no simple solution has been worked out. The only difficulty is the solution of many simultaneous linear equations. A general case of three phase equilibrium for example would lead to a solution of 40 000 terms. Simplifications, however, are to be expected especially if theoretical constants are used.

e. The double carbides theta ($Co_3W_6C_2$) and kappa ($Co_3W_{10}C_4$), revealed in this work, have been shown to exist as individual phases. The lattice symmetry is simple but the large unit cells suggest complicated structures. It is estimated that the unit cell of the theta phase will contain more atoms than the unit cell of eta, 112,[29] and even the unit cell of the kappa phase must contain about 34 atoms. The eta structure contains units of structure, which are identical with the diwolfram carbide structure. It would seem very probable that this unit would be preserved in the intermediate theta and kappa phases.

f. There is considerable speculation involved in the construction of the ternary diagram models. The principle was to study the isothermal section at 1400°C and based on that and the known binaries, predict the reactions, which occur at high temperatures. After the main features of the diagram were understood, more detailed study was carried on on points of greater importance. Many of the conclusions have been obtained by the ternary phase theory rather than by experiment. It is pointed out that the work is of tentative nature and supposed to serve as a guide for further study rather than a completed work.

g. The two diagrams, stable and metastable, had to be postulated to explain the two completely different structures found in one specimen, as explained on page 57. The equilibrium eta-graphite has been reported many times, first by Wyman and Kelley[23]. On the other hand the cobalt cemented carbides normally consist of beta and WC phases although the cooling rates applied are not too fast.

h. It is believed that the reactions in the sintering of the cemented carbides can be understood only by means of the ternary equilibria. The quasi-binary diagram cobalt-WC, usually assumed is not correct.

The narrow two phase field beta-WC and the relatively small temperature difference of 60°C between the invariant reactions, liquid = beta + WC + graphite and liquid + eta = beta + WC, indicate the critical conditions present in the sintering. If eta phase forms during cooling from the sintering temperature depends on whether or not the invariant plane of liquid - eta - beta - WC equilibrium extends over the two phase field beta + WC. So far this has not been determined although the composition of the saturated liquid is closely encircled.

Both eta and graphite will deteriorate the properties of the cemented carbides and therefore fast cooling rates are necessary to avoid the stable equilibria.

12. Suggestions for Further Work

Many of the results of this study are of tentative nature and require continuous study. In the following only such subjects are pointed out, which are believed to be of vital importance.

From the viewpoint of technical applications, the neighborhood of the section cobalt-WC requires clarification. The composition of the saturated liquid at the peritectic reaction liquid + eta = beta + WC should be determined by thermal analysis, because it determines whether or not eta phase forms during the sintering operation of the cemented carbides.

Theoretically interesting would be the solution of the structure of the new double carbides, theta and kappa. These carbides together with W_2C and eta form a series of interesting structures, which contain identical structural units.

The new x-ray method to evaluate phase boundary compositions has shown to be versatile. The application for ternary diagrams remains to be solved. On the other hand the segregation of the phases in x-ray specimens should be studied both theoretically and experimentally. This type of study probably would reveal new applications of the method.

Biographical Sketch

The author, Pekka Rautala, was born in Uusikaupunki, Finland, on April 16, 1918.

He attended schools in Helsinki, where the secondary schooling was received at the Normal School.

He matriculated at the Helsinki University in September 1938 and enrolled the next year at the Helsinki Institute of Technology. The studies were interrupted by the war. After four years of service in the Finnish Army, where he was promoted to the rank of First Lieutenant, the author returned to the Helsinki Institute of Technology and was graduated with the degree of Bachelor of Science in October 1946.

After one term as a teaching assistant in Metallurgy at the Helsinki Institute of Technology, the author was employed as a process engineer at Imatra Steelworks, Finland.

He enrolled at the Massachusetts Institute of Technology in September, 1948. In February, 1949 he was appointed research assistant and in September, 1950, instructor in the Department of Metallurgy.

He is a member of engineering societies in Finland and of the Society of the Sigma Xi.

Bibliography

1. L. D. Brownlee, The Ternary System Tungsten-Carbon-Cobalt, Unpublished Report, Vickers Electrical Company, Ltd. Manchester, England.

2. W. P. Sykes, A Study of the Tungsten-Carbon System. Trans. Am. Soc. Steel Treating, 18, (1930) 268

3. Metals Handbook, (1948) Edition, Am. Soc. of Metals, Cleveland, 1180, 1184 and 1193.

4. O. Ruff and F. Keilig, Arbeiten im Gebiete hoher Temperaturen VIII. Kobalt und Kohlenstoff, Z. anorg. Chem. 88, (1914) 410.

5. R. Schenck and H. Klas, Gleichgewichtsuntersuchungen ueber die Reduktions - Oxydations und Kohlungsvorgange beim Eisen VII, Kobalt unter einer Methan Wasserstoffatmosphare, Z. anorg. u. allgem. Chem. 178, (1929) 146

6. L. J. E. Hofer and W. C. Peebles, Preparation and X-ray Diffraction Study of a New Cobalt Carbide. J. Am. Chem. Soc. 69, (1947) 893

7. H. A. Bahr and V. Jensen, Die Kohlenoxydspaltung am Kobalt, Ber. 63 (1930) 2226

8. G. Boecker, Untersuchungen ueber das System Kobalt - Kohlenstoff. Metallurgie 9, (1912) 296

9. S. Takeda, A Metallographic Study of the Action of the Cementing Material for Cemented Tungsten Carbide. Science Repts. Tohoku Imp. Univ. Hondu Anniversary Volume, (1936) 864.

10. W. P. Sykes, The Cobalt-Tungsten System. Trans. Am. Soc. Steel Treating 21, (1933), 385.

11. W. Koester and W. Tonn, Die Zweistoffsysteme Kobalt-Wolfram und Kobalt-Molybdaen, Z. Metallkunde 24, (1932) 296.

12. A. Magneli and A. Westgren, Roentgenuntersuchung von Kobalt-Wolframlegierungen; Z. anorg. u. allgem. Chem. 238, (1938) 268.

13. P. Williams, Sur la Preparation et les Proprietes d'un Nouveau Carbure de Tungstene, Compt. Rend. 126, (1897), 1732.

14. H. Moissan, Recherches sur le Tungstene, Compt. Rend. 123, (1896), 15.

15. A. Westgren and G. Phragmen, Roentgenanalyse der Systeme Wolfram-Kohlenstoff und Molybdaen - Kohlenstoff. Z anorg. u. allgem. Chem. 156, (1926), 27.

16. K. Becker, Die Kristallstruktur und der Lineare Waermeausdehnungskoeffizient der Wolframcarbide. Z. Physik 51, (1928), 481.

17. C. W. Horsting, Carbide Structures in Carburized Thoriated - Tungsten Filaments. J. Applied Phys. 18, (1947), 95.

18. V. Adelskold, A. Sundelin and A. Westgren, Carbide in kohlenstoffhaltigen Legierungen von Wolfram und Molybdaen mit Chrom, Mangan, Eisen, Kobalt und Nickel, Z. anorg. u. allgem. Chem. 212, (1933), 401.

19. S. Takeda, On the carbides in Tungsten Steels. Technol Repts Tohoku Imp. Univ. 9 (1931) 483, 627 and 10 (1931) 42.

20. E. N. Kislyokova, Zhur. Fiz. Khim. 17, (1943), 108.

21. E. J. Sandford and E. M. Trent, The Physical Metallurgy of Sintered Carbides. Iron Steel Inst. Symposium on Powder Metallurgy, Special Report 38, (1947) 84.

22. H. Franssen, Gefuege von Hartmetall-Legierungen. Arch. Eisenhuettenw. 19, (1948), 79.

23. L. L. Wyman and F. C. Kelley, Cemented Tungsten Carbide - A Study of the Action of the Cementing Material. Trans. Am. Inst. Mining Met. Engrs. 93, (1931), 208.

24. Krupp Widia Works, U.S. Dept. Comm. P.B. F.I.A.T. Microfilm Reel No. 56. Krupp Widia Report No. 133, Frames 2198 - 2200.

25. M. U. Cohen, Precision Lattice Constants from X-ray Powder Photographs. Rev. Sci. Instruments 6, (1935), 68.

26. A.Mimeographed Resume of Lectures Given by Professor B. Warren at Massachusetts Institute of Technology, 29.

27. H. J. Goldschmidt, The Structures of Carbides in Alloy Steels. J. Iron Steel Inst. 160, (1948), 345.

28. O. Ruff and R. Wunsch, Arbeiten im Gebiete hoher Temperaturen III. Wolfram und Kohlenstoff, Z. anorg. Chem. 85, (1914), 294.

29. A. Westgren, Snabbstalskarbidens Kristallstruktur, Jernkontorets Ann. 117, (1933), 1.

30. A. Taylor, An Introduction to X-ray Metallography, Chapman and Hall Ltd. London (1945), 331-391.

Appendix I

Sample Calculation of Symmetrical Focussing Camera Film

Specimen: 32.5 atomic percent carbon

Sintering temperature: 2000°C

Radiation: Cobalt K alpha

Notation: S = distance between symmetrical lines on film

$\varphi = 90° - \theta$

$\alpha = h^2 + hk + k^2$

$\gamma = l^2$

$\delta = 5 \phi \sin\phi$, where $\phi = 2\varphi$

$v = \sin^2\theta_a - \sin^2\theta$, where $\sin^2\theta_a$ is calculated from approximate lattice constants.

h k l	Radiation	S, mm	S, av. mm.
1 2 1	α_1	151.30, 151.35, 151.30	151.32
	α_2	149.20, 149.15, 149.20	149.18
1 1 4	α_1	109.60, 109.65, 109.65	109.63
	α_2	106.45, 106.45, 106.45	106.45
1 2 2	α_1	65.75, 65.75, 65.75	65.73
	α_2	60.10, 60.05, 60.15	60.10

deg.	deg.	Sin θ	$Sin^2\theta$	$Sin^2\theta_c$
21.3799	68.6201	.931 183 7	.867 103	.869 10
21.0776	68.9224	.933 094 2	.870 665	.866 89
15.4896	74.5104	.963 679 0	.928 677	.928 68
15.0403	74.9597	.965 742 6	.932 661	.928 62
9.2870	80.7130	.986 892 4	.973.957	.973 96
9.4915	80.5085	.989 037 8	.978 196	.973 96

h k l	$\sin^2\theta_a$	v	δ
12.1	.87000	.00300	2.536
11.4	.93170	.00305	1.389
12.2	.97770	.00374	.516
	$\alpha\delta$	$\gamma\delta$	δ^2
12.1	17.752	2.536	6.4313
11.4	4.167	22.224	1.9293
12.2	3.612	2.064	.2663
	25.531	26.824	8.6269
	αv	γv	δv
12.1	.02100	.00300	.00761
11.4	.00915	.04880	.00424
12.2	.02618	.01496	.00193
	.05633	.06676	.01378

$$
\begin{aligned}
107.000\ \Delta A + 83.000\ \Delta C + 25.5310\ \Delta D &= .05633 \\
83.000\ \Delta A + 273.000\ \Delta C + 26.8240\ \Delta D &= .06676 \\
25.531\ \Delta A + 26.824\ \Delta C + 8.6269\ \Delta D &= .01378
\end{aligned}
$$

$$
\Delta A = \frac{\begin{vmatrix} .05633 & 83.000 & 25.5310 \\ .06676 & 273.000 & 26.8240 \\ .01278 & 26.824 & 8.6269 \end{vmatrix}_1}{\begin{vmatrix} 107.000 & 83.000 & 25.5310 \\ 83.000 & 273.000 & 26.8240 \\ 25.531 & 25.824 & 8.6269 \end{vmatrix}_2}
$$

The expansion of the determinants 1 and 2 is:

132.665 245	40.530 955
30.679 682	47.802 343
45.720 155	96.046 090
209.065 082	184.379 388
184.379 388	
24.685 694	

252 000.376	76 989.387
56 842.014	59 430.714
56 842.014	177 950.125
365 684.404	314 370.226
314 370.226	
51 314.178	

$$\Delta A = \frac{24.685\ 694}{51\ 314.178} = 4.8107 \times 10^{-4}$$

$$\Delta C = \frac{\begin{vmatrix} 107.000 & .05633 & 25.5310 \\ 83.000 & .06676 & 26.8240 \\ 25.531 & .01378 & 8.6269 \end{vmatrix}_3}{\begin{vmatrix} & & \\ & & \\ & & \end{vmatrix}_2}$$

The expansion of the determinant 3 is:

61.624.707	43.516 302
38.577 237	40.334 122
29.200 826	39.550 915
129.402 770	123.401 339
123.401 339	
6.001 431	

$$\Delta C = \frac{6.001\ 431}{51\ 314.178} = 1.1695 \times 10^{-4}$$

A_a = .119159	C_a = .035 888 2
ΔA = .000481	ΔC = .000 117 0
A = .118678	C = .035 771 2

$\lambda^2/3 = 1.066\ 721$; $\lambda^2/4 = .800\ 040\ 8$

$$\therefore\ a^2 = \frac{1.066\ 721}{.118\ 678} = 8.988\ 363 \qquad c^2 = \frac{.800\ 040\ 8}{.035\ 7712} = 22.365\ 50$$

and therefore the lattice constants are:

$$a = \underline{2.9981\ A} \qquad c = \underline{4.7292\ A}$$

$$c/a = \underline{1.5774}$$

Appendix II

Solution of Equations (7)

The intensity ratio vs. composition curve is a hyperbola. Because of the accidental errors , the equation (6) is not fulfilled by the experimental values. The equation for each point will be:

$$z\,(b_2 - b) - r\,(b - b_1) = \Delta$$

which differs from equation (6) by the term Δ. By squaring and summing the Δ's one gets

$$\Sigma\Delta^2 = \Sigma\left[\, z^2\,(b_2 - b)^2 - 2rz(b_2 - b)(b - b_1) + r^2\,(b - b_1)^2\right]$$

Differentiation of this equation with respect to the unknown constants, b_1 and b_2, and equating these to zero gives:

$$\frac{\partial(\Sigma\Delta^2)}{\partial b_1} = \Sigma\left[z(b_2 - b) - r\,(b - b_1)\right] = 0$$

$$\frac{\partial(\Sigma\Delta^2)}{\partial b_2} = \Sigma\left[z^2(b_2 - b) - rz(b - b_1)\right] = 0$$

which equations can be simplified to:

$$n\,r\,b_1 + \Sigma z \cdot b_2 = \Sigma bz + r\Sigma b$$

$$\Sigma z \cdot rb_1 + \Sigma z^2 \cdot b_2 = \Sigma bz^2 + r\Sigma bz$$

where n is the number of the experimental points. The solutions of these equations are in determinant form:

$$b_1 = \frac{\begin{vmatrix} \Sigma bz + r\Sigma b & \Sigma z \\ \Sigma bz^2 + r\Sigma bz & \Sigma z^2 \end{vmatrix}}{\begin{vmatrix} rn & \Sigma z \\ r\Sigma z & \Sigma z^2 \end{vmatrix}}$$

$$b_2 = \frac{\begin{vmatrix} n & \Sigma bz + r\Sigma b \\ \Sigma z & \Sigma bz^2 + r\Sigma bz \end{vmatrix}}{\begin{vmatrix} n & \Sigma z \\ \Sigma z & \Sigma z^2 \end{vmatrix}}$$

Evaluation of these determinants gives the solutions (8). Solutions (8a) are obtained in principle the same way.

Appendix III

Derivation of Graphical Solution

The point of tangency is called b_o, z_o. If the slope of the curve is equal to one, the distance to the vertical assymptote b_2 is $b_2 - b_o$. The distance to the horizontal assymptote is $z_o + r$. These two distances are equal:

$$b_2 - b_o = z_o + r$$

and therefore

$$b_2 = b_o + z_o + r$$

which is the second equation (9)

The slope of hyperbola (6) is:

$$\frac{dz}{db} = r \frac{b_2 - b_1}{(b_2 - b)^2}$$

and when the slope is unity:

$$r \frac{b_2 - b_1}{(b_2 - b_o)^2} = 1$$

Substituting $b_2 - b_o = z_o + r$ and squaring one gets

$$b_1 = (b_2 - r - z_o) - z_o - z_o^2/r$$

but $b_2 - r - z = b_o$

$$\therefore b_1 = b_o - z_o - z_o^2/r$$

which is the first equation (9).

Appendix IV

Calculations of Theorectical r

By equation (5) r is a function of structure factors, multiplicities etc. The structure fact FF* can be evaluated by equation:

$$F = \Sigma f \exp.\left[2\pi i \quad (hx + ky + lz)\right]$$

where f is the atomic scattering factor and x, y and z the coordinates of the atoms, F* is the conjugate complex to F.

Multiplicities depend on indeces (h,k, l) and the Loretz - Polarization factor is a function of the line position only. The volume of the unit cell is obtained from the lattice constants. Tables given in reference (30) have been used, except for the wavelengths and the lattice constants.

W - WC system

In WC the wolfram and carbon atoms occupy positions [15]:

$$W: \quad x = o, \quad y = o, \quad z = o$$

$$C: \quad x = 1/3, \quad y = 2/3, \quad z = \tfrac{1}{2}$$

Therefore $F_{wc} = f_w + f_c \qquad \exp\left[2\pi i(h/3 + 2h/3 + l/2)\right.$

$$\therefore FF^*_{wc} = f_w^2 + 2 f_w f_c \cos 2\pi (h/3 + 2k/3 + l/2) + f_c^2$$

In wolfram the atoms are in positions

$$W: \quad x = o, \quad y = o, \quad z = o$$

$$W: \quad x = \tfrac{1}{2}, \quad y = \tfrac{1}{2}, \quad z = \tfrac{1}{2}$$

Therefore $F_w = f_w \left[1 + \exp.\left\{ 2\pi i(h/2 + k/2 + l/2)\right\}\right]$

$$\therefore FF^*_w = 2f_w^2 \left[1 + \cos \pi (h+k+l)\right]$$

For 10.1 and 110 reflections one gets

$$FF^*_{wc_{10.1}} = f_w^2 + f_w f_c + f_c^2 = 55.1^2 + 55.1 \times 2.4 + 2.4^2 = 3174$$

$$FF^*_{w_{110}} = 4f_w^2 = 4 \cdot 58.4^2 = 13642$$

The multiplicities in this case are both equal:

$$j_{wc_{10.1}} = 12 \qquad j_{w_{110}} = 12$$

The Lorentz - Polarization factors are

$$(L.P.)_{wc_{10.1}} = 18.92 \qquad (L.P.)_{w_{110}} = 28.42$$

and the volumes of the unit cells:

$$Va_{wc} = \frac{\sqrt{3}}{2} a^2 \cdot c = \frac{\sqrt{3}}{2} \cdot 2,9062^2 \cdot 2.8335 = 20.73 \ A^3, \text{ and}$$

$$Va_w = a^3 = 3.1644^3 = 31.69 \ A^3$$

The molecular weights of WC and W are 195.9 and 379.9 respectively.

Substitution of all these values into equation (5) gives:

$$r = \frac{3174 \times 12 \times 18.92 \times 31.69 \times 367.6}{13642 \times 12 \times 28.42 \times 20.73 \times 195.9} = .444$$

For 11.2 and 310 reflections it is obtained similarily: r = .399

and for 30.1 and 321 reflections: r = .245

<u>W_2C - WC System</u>

The values for WC have been calculated above.

According to Becker[16], W_2C has C - atoms at zero positions

and W - atoms in positions 1/3, 2/3, 1/3.71; 2/3, 1/3, 1/1.37

Therefore

$$F_{W_2C} = f_c + f_w \left[\exp. \left\{ 2\pi i(h/3 + 2k/3 + 1/3.71) \right\} + \exp \left\{ 2\pi i(2h/3 + k/3 + 1/1.37) \right\} \right]$$

$$FF^*_{W_2C} = f_c^2 + 2f_c f_w \left[\cos 2\pi(h/3 + 2k/3 + 1/3.71) + \cos 2\pi(2h/3 + k/3 + 1/1.37) \right]$$

$$+ 4 f_w^2 \cos^2 \pi (h/3 - k/3 + 1/2.175)$$

For 10.1 reflection one gets

$$FF^*_{W_2C_{10.1}} = f_c^2 - 3.1912\, f_c f_w + 2.534\, f_w^2 = 8215$$

The Lorentz - Polarization factor for $W_2C_{10.1}$ is 29.66 and the volume of the unit cell

$$Va_{W_2C} = \frac{\sqrt{3}}{2} a^2 c = \frac{\sqrt{3}}{2} \cdot 2.9978^2 \times 4.7290 = 36.80\ A^3$$

Substition into equation (5) gives:

$$r = \frac{3174 \times 12 \times 18.92 \times 36.80 \times 379.8}{8215 \times 12 \times 29.66 \times 20.73 \times 195.9} = .848$$

Appendix V

Solubility Limits of W_2C and WC

Calculations by equation (8)

The value of r, needed in these calculations, has been evaluated in Appendix IV to .848. The experimental results of Table VIII are used.

b	z	bz	z^2	bz^2
3.68	.2586	.951 648	.066 874	.246 096
4.19	.5437	2.278 103	.295 610	1.238 605
4.57	.8847	3.860 279	.713 518	3.260 778
5.13	1.7032	8.737 416	2.900 890	14.881 567
17.57	3.3502	15.827 446	3.976 892	19.627 046

$\therefore \Sigma b = 1757 \qquad \Sigma z = 3.3502 \qquad \Sigma bz = 15.827\ 446$

$\Sigma z^2 = 3.976\ 892 \qquad \Sigma bz^2 = 19.627\ 046$

$\Sigma bz = 15.827\ 446$

$r\Sigma b = 14.899\ 36$

$30.726\ 806 \times \Sigma z^2 = 122.197\ 189$

$\Sigma bz^2 = 19.627\ 046$

$r\Sigma bz = 13.421\ 674$

$33.048\ 720 \times \Sigma z = 110.719\ 822$

$11.477\ 367$

$n\Sigma z^2 = 15.907\ 568$

$15.907\ 568 \times r = 13.489\ 618$

$(\Sigma z)^2 = 11.223\ 840$

$11.223\ 840 \times r = 9.517\ 816$

$3.971\ 802$

$$b_1 = \frac{11.477\ 367}{3.971\ 802} = 2.889\ 7 \text{ wt. percent} = 31.302 \text{ atomic percent}$$

$$b_2 = \frac{n \times 33.048\ 720 - \Sigma z \times 30.726\ 806}{15.907\ 568 - 11.223\ 840}$$

$$= \frac{29.253\ 935}{4.683\ 728} = \underline{6.245\ 9} \text{ wt. percent} = \underline{50.498} \text{ atomic percent}$$

Calculations by equations (8a)

In addition to the sums formed above, two more sums have to be calculated:

$$\Sigma b^2 = 78.300\ 300$$

$$\Sigma b^2 z = 75.511\ 736$$

The calculations by equations (8a) are:

$$\Sigma z \Sigma b^2 z = 252.979\ 418$$

$$(\Sigma bz)^2 = \underline{250.508\ 046}$$

$$-2.471\ 371 \times \Sigma bz = -39.115\ 493$$

$$\Sigma bz\ \Sigma bz^2 = 310.646\ 011$$

$$\Sigma z^2\ \Sigma b^2 z = \underline{300.302\ 019}$$

$$-10.343\ 992 \times \Sigma b = \underline{-181.743\ 939}$$

$$-220.859\ 432$$

$$\Sigma z\ \Sigma bz^2 = 65.753\ 529$$

$$\Sigma bz\ \Sigma z^2 = \underline{62.944\ 043}$$

$$+2.810\ 486 \times \Sigma b^2 = \underline{220.061\ 905}$$

$$-.797\ 627$$

$$-2.471\ 371 \times \Sigma z = -8.279\ 587$$

$$-10.343\ 922 \times n = \underline{-41.375\ 968}$$

$$-49.655\ 555$$

$$2.810\ 486 \times \Sigma b = \underline{49.380\ 241}$$

$$-.275\ 314$$

$$b_1 = \frac{-.797\ 527}{-.275\ 314} = \underline{2.8958} \text{ wt. percent} = \underline{31.356} \text{ atomic percent}$$

$\Sigma bz \; \Sigma b$ = 278.088 226

$\Sigma z \; \Sigma b^2$ = 262.321 665

- 15.766 561 x Σbz = - 249.544 393

$n \; \Sigma b^2$ = 313.201 200

$(\Sigma b)^2$ = 308.704 900

- 4.496 300 x Σbz^2 = - 88.249 087

- 337.793 479

$n \; \Sigma bz$ = 63.309 784

$\Sigma z \Sigma b$ = 58.863 014

4.446 770 x $\Sigma b^2 z$ = 335.783 322

- 2.010 157

- 15.766 561 x Σz = - 52.821 136

- 4.496 300 x Σz^2 = - 17.881 299

- 70.702 435

- 4.446 300 x Σbz = 70.381 012

- .321 423

$b_2 = \frac{-2.010\ 157}{-\ .321\ 423} = \underline{6.2539}$ wt. percent = $\underline{50.532}$ atomic percent

$r = \frac{-\ .275\ 314}{-\ .321\ 423} = \underline{.857}$

Appendix VI

Thermal Analysis Technique

The thermal analysis were made by the inverse rate method. The powder mixtures were melted in an alundum crucible by induction heating. When a temperature of about 1750°C was reached, the power was shut off and a platinum-rhodium thermocouple was inserted into the melt.

The electromotive force was measured by a regular potentiometer called here potentiometer A, but the galvanometer was replaced by a sensitive General Electric recording potentiometer, called potentiometer B, which had a full scale deflection of .2 mv. This setup eliminated the use of stop watches and the delays due to galvanometer oscillations, because the recording potentiometer was excellently damped.

The main dial of the potentiometer A was set to reading, from which the analysis was started. The potentiometer B then exceeded its scale, but during cooling approached the zero line. When this was reached the dial of potentiometer A was turned in one .1 mv step, which caused an immediate response of the pointer of potentiometer B to .1 mv line and back toward zero again. This cycle was repeated over the whole temperature range.

The distance between the subsequent steps on recorder chart is directly proportional to the time needed for cooling by a temperature interwall, which corresponds to .1 mv. The cooling curves in Figure 7 were obtained by plotting the setting of potentiometer A versus the length of the previous step on the chart of potentiometer B.